Newsletter of the Climate Variability and Predictability Programme (CLIVAR)

Exchanges

No. 33 (Vol 10, No.2) April 2005

From Hill, Page 3: The importance of the assembly of global ocean datasets: the role of the CLIVAR Data Assembly Centres (DACS)

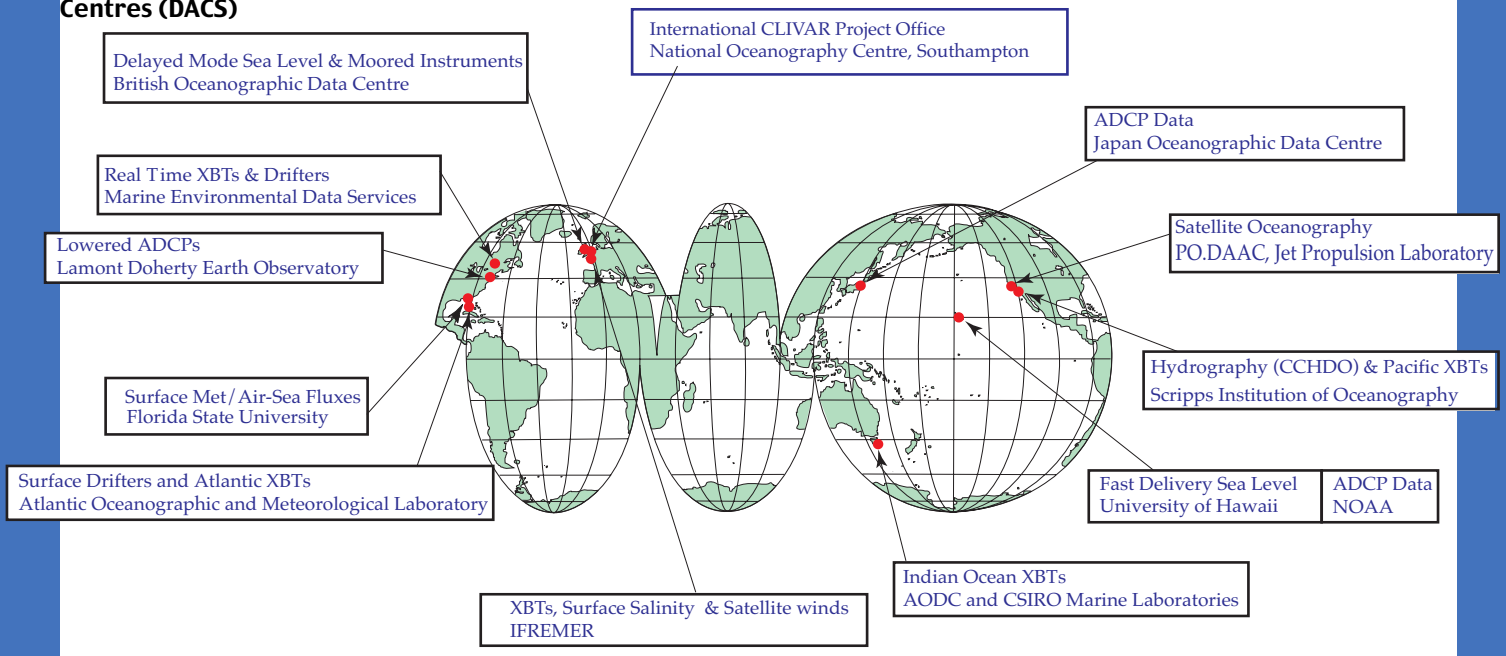

Figure 1 CLIVAR Data Assembly Centers

CLIVAR is an international research programme dealing with climate variability and predictability on time-scales from months to centuries.

WCRP

CLIVAR is a component of the World Climate Research Programme (WCRP). WCRP is sponsored by the World Meteorological Organization, the International Council for Science and the Intergovernmental Oceanographic Commission of UNESCO.

Latest CLIVAR News **http://www.clivar.org/recent/**

See the CLIVAR Calendar *http://www.clivar.org/calendar/index.htm*

This issue has been sponsored by the China Meteorological Administration through the Chinese Academy of Meteorological Sciences

Call for Contributions

We would like to invite the CLIVAR community to submit papers to CLIVAR Exchanges for issue 35. The overarching topic will be on **The Southern Ocean Region and The International Polar Year.** The deadline for this issue will be July 31st 2005.

Guidelines for the submission of papers for CLIVAR Exchanges can be found under: http://www.clivar.org/publications/exchanges/guidel.htm

Editorial

Enclosed with this issue of Exchanges is a copy of a flyer outlining the new WCRP COPES initiative. COPES stands for "Coordinated Observation and Prediction of the Earth System" and is WCRP's new strategy for managing all of the activities that come under the WCRP umbrella. It is important to note that COPES is **not** another WCRP project in the sense that CLIVAR, GEWEX, SPARC and CliC are, but a framework against which the various contributions from WCRP's projects contribute. Indeed, the projects are essential to delivery of the COPES strategy. A COPES Task Team met in January 2005 to formulate the *modus operandi* of COPES. In consequence, COPES was a major topic the 26th meeting of the Joint Scientific Committee (JSC) for WCRP held in Guayaquil, Ecuador from 14-18 March 2005, to the discussion of which CLIVAR brought constructive but critical and challenging feedback for the JSC to consider.

As well as COPES, JSC 26 also considered a number of other areas of key interest to CLIVAR. As part of the new way of doing business under COPES, the JSC reviewed overall WCRP progress and strategy in a number of overarching areas, all of relevance to CLIVAR. These covered (i) WCRP monsoon research overall, under which CLIVAR and GEWEX are co-sponsoring and organising the first pan-WCRP Workshop on the Monsoon Climate Systems (Irvine, California, 15-17 June 2005) to further develop the strategy for this area under WCRP; (ii) atmospheric chemistry and climate, a topic for which the JSC decided to establish a new Task Force (in which CLIVAR will be involved) to develop a road map for chemistry-climate models, observations and process studies; (iii) sea level rise which, the JSC agreed, will be the topic of a major WCRP Workshop next year and (iv) anthropogenic climate change, for which the JSC decided to develop an inventory of activities and future roadmap, to be considered by JSC 27 and to which CLIVAR will be a major contributor.

Overall progress with CLIVAR, presented by CLIVAR Co-Chair Tony Busalacchi, was well received by the JSC. The JSC endorsed the decision by CLIVAR's SSG-13 to follow a four-science theme approach in CLIVAR focussed on (a) ENSO, (b) monsoons, (c) decadal variability and the thermohaline circulation and (iv) anthropogenic climate change. At the same time, the JSC re-emphasised CLIVAR's predominant role in WCRP to address the overall role of the oceans in climate.

For the first time in a while, this edition of CLIVAR Exchanges contains a variety of articles, not linked to a specific theme of CLIVAR research, though a number of the papers are linked to the issue of seasonal prediction, the theme of our last issue. I would draw particular attention to the first article of this issue, by Katy Hill, which deals with the issue of ocean data management in CLIVAR and in particular the role of the CLIVAR Data Assembly Centres (DACs). If you are involved in ocean measurements, you are strongly encouraged to submit data to them as appropriate so as to help build the database of CLIVAR-relevant data, make your data available to the wider community and facilitate its use in climate analyses and ocean reanalysis in particular.

Ocean reanalysis was the subject of a major CLIVAR Workshop last November. The workshop, which was held in Boulder with Kevin Trenberth acting as host, brought together a broad spectrum of expertise in this area with over 80 attendees. The outcomes of the Conference were reviewed at the meeting of CLIVAR's Global Synthesis and Observations Panel (GSOP) which followed it and which was co-chaired by Dean Roemmich and Detlef Stammer. As well as how to move forward with ocean reanalysis, GSOP also considered the range of ocean observations and how best to move forward with aspects of CLIVAR data management. One of the outcomes was a firming up of the CLIVAR data policy, printed on pages 4 and 5 of this edition of Exchanges.

Both the GSOP meeting and the Reanalysis Workshop were staffed from the ICPO by Katy Hill who left us this month in order to take up the offer of a Ph.D studentship in Hobart where she will be working, amongst others, with Steve Rintoul. Katy joined us in November 2002 and over the period that she has been with us has developed into an experienced member of the ICPO staff, responsible for CLIVAR's Pacific Panel and GSOP, hydrography and carbon links and aspects of CLIVAR data management. We will much miss her expertise and lively way of doing things but wish her well for the future both in her new life in Hobart and in her Ph.D studies. Antonio Caetano Caltabiano (otherwise known as Nico) has joined the ICPO as Katy's replacement initially on a short-term contract to the end of June. Nico, who is originally from Brazil, has a degree in Oceanography, a masters in remote sensing and applications and has'recently finished his PhD in oceanography here at SOC. His PhD involved him in use of remote sensing and PIRATA and other data in studies of tropical instability waves. He also took part in the first Brazilian cruise for PIRATA mooring deployment. Over recent months he has worked at SOC on validation and scientific use of ENVISAT radar altimeter data and is now settling into his new role here at the ICPO. Welcome Nico.

Howard Cattle

National Oceanography Centre, Southampton
UNIVERSITY OF SOUTHAMPTON AND NATURAL ENVIRONMENT RESEARCH COUNCIL

PLEASE NOTE: As from 1st May 2005, The Southampton Oceanography Centre has become **The National Oceanography Centre, Southampton.** The email address is now: **icpo@noc.soton.ac.uk**

The importance of the assembly of global ocean datasets: the role of the CLIVAR Data Assembly Centres (DACs)

Katy Hill, ICPO, Southampton, United Kingdom
Corresponding author: icpo@noc.soton.ac.uk

Ocean observations are a key element of the CLIVAR programme. CLIVAR aims to help establish the appropriate mix of measurement platforms and synthesis techniques required to determine the full suite of ocean variables, including air-sea fluxes. Coordinated global collation and quality control of key data streams is essential. Accessing and searching these data is even more critical. CLIVAR is initiating plans to address these needs. As a general policy, CLIVAR encourages the timely and open exchange of data relevant to the programme's mission. Submission of data to official CLIVAR DACs, national archives and other data centres that support CLIVAR's mission, is strongly encouraged (see CLIVAR's Data Policy on page 4). For ocean observations, CLIVAR has enlisted the support of a number of Data Assembly Centres (DACs) dedicated to the collation and archival of ocean data as well as the delivery of data and products (Figure 1, front cover and below). To date there have been a number of scientific cruises and experiments for which data have been recorded, but perhaps not made publicly available. Please make the most of these specialized DACs and help produce the necessary products for climate research by providing relevant data to them. For general observation related enquiries, do not hesitate to contact the International CLIVAR Project Office at icpo@noc.soton.ac.uk

---

ADCP DACs

ADCP Data Archive at the Japan Oceanographic Data Centre (JODC)
Principal Contact: Nobuyuki Shibayama mail@jodc.go.jp
Website: http://www.jodc.go.jp/goin/adcp.html

Hawaii Joint Archive for Shipboard ADCP (JASADCP)
Principal Contact: Patrick Caldwell caldwell@hawaii.edu
Website: http://ilikai.soest.hawaii.edu/sadcp/
Joint Responsibilities: Shipboard ADCP data.
The co-DACs seek out CLIVAR principal investigators and data contacts for calibrated and quality-controlled shipboard ADCP datasets.

CLIVAR LADCP DAC, Lamont-Doherty Earth Observatory, USA
Principal contact: Andreas Thurnherr ant@ldeo.columbia.edu
Website: http://ladcp.ldeo.columbia.edu/ladcp/clivar/
Responsibilities: Lowered ADCP Data. To collect (shared responsibility with E. Firing), process and make available the LADCP data from CLIVAR cruises.

Drifter DACs (Surface Velocity program)

Marine Environmental Data Service, Fisheries and Oceans Canada (real time)
Principal Contact: J. Robert Keely keeley@meds-sdmm.dfo-mpo.gc.ca
Website: http://www.meds-sdmm.dfo-mpo.gc.ca/MEDS/Databases/DRIBU/drifting_buoys_e.htm

Physical Oceanography Division, NOAA-AOML (delayed mode)
Principal contact: Mayra Pazos, pazos@aoml.noaa.gov
Website: http://www.aoml.noaa.gov/phod/dac/gdc.html
Joint Responsibilities: AOML receives, assembles, processes and applies quality control to the data received by AOML and at Service ARGOS from national and international partners. MEDS acts as the archive and distributor of the data. In this latter respect, MEDS also holds the original data that circulated in real-time and some delayed mode data acquired directly from PIs.

Hydrographic DAC

CLIVAR/Carbon Hydrographic Data Office (CCHDO).
Principal Contact : Jim Swift whpo@ucsd.edu
Website: http://whpo.ucsd.edu
Responsibilities: Formerly the WOCE Hydrographic Project Office, CCHDO collects and manages all hydrographic (ship based) data related to CLIVAR. This includes WOCE hydrographic programme data, CLIVAR repeat hydrography data, global ocean carbon hydrographic data and other similar CTD/hydrographic data.

Moored Instrument DAC

British Oceanography Data Centre
Principal Contact: Mary Mowat mmow@bodc.ac.uk
Website: http://www.bodc.ac.uk/projects/clivar/
Responsibilities: BODC is responsible for delivering delayed mode moored instrument data for CLIVAR. This will include mainly current meters and ADCPs, but other types of moored instrument such as thermistor chains and sediment traps may also be included. The aim is to assemble a uniformly-processed and quality controlled set of CLIVAR deep water moored instrument records. BODC also runs the Delayed Mode Sea Level DAC.

Satellite DACs

PO.DAAC
Contact: Jorge Vazquez jv@pacific.jpl.nasa.gov
Website: http://podaac.jpl.nasa.gov/
Responsibilities: To archive and distribute satellite oceanography data.

Satellite Winds DAC

CERSAT (French ERS Processing and Archiving Centre), IFremer, France

Principal Contact: Jean-Francois Piole.
Jean.Francois.Piolle@ifremer.fr
Website: http://www.ifremer.fr/cersat
Responsibilities: CERSAT delivers global mean wind fields derived from various scatterometers (ERS-1, ERS-2, NSCAT, QuikSCAT). It is bringing new products such as high frequency blended wind fields (merging scatterometer, altimeter, radiometer and model outputs data) and fluxes derived from satellite observations (latent heat).

Sea Level DACs

Fast Delivery: **The Sea Level Data Centre**
Principal Contact: Bernie Kilonsky: kilonsky@soest.hawaii.edu
Website: http://uhslc.soest.hawaii.edu

Delayed Mode: **British Oceanography Data Centre**
Principal Contact: Elizabeth Bradshaw elizb@bodc.ac.uk
Website: http://www.bodc.ac.uk
Responsibilities: The Sea Level Data Center at the University of Hawaii provides "fast delivery" in-situ sea level data at sites identified by the Global Sea Level Observing System (GLOSS). BODC delivers delayed mode sea level data and maintains the joint archive for Sea Level Research Quality data.

Surface Marine Meteorology DAC

Surface Marine Meteorological Data Assembly Center, Center for Ocean-Atmospheric Prediction Studies, Florida State University.
Principal Contact: Shawn R. Smith smith@coaps.fsu.edu
Website: http://www.coaps.fsu.edu/RVSMDC/CLIVAR/
Responsibilities: To collect, quality control, distribute, and assure archival of underway surface meteorological observations from CLIVAR hydrographic cruises. Additional surface meteorology data will be accepted from CLIVAR-sponsored experiments in the marine environment. We anticipate data submissions from research vessels and moored buoys that are either observed by nearly-continuous recording systems or ship bridge officers.

Upper Ocean Thermal DACs

Marine Environmental Data Service, Fisheries and Oceans, Canada
Principal Contact: J. Robert Keely keeley@meds-sdmm.dfo-mpo.gc.ca
Website: http://www.meds-sdmm.dfo-mpo.gc.ca/meds/Databases/OCEAN/Realtime_e.htm

Global Subsurface Data Center, IFREMER, France
Principal Contact: Loic Petit de la Villeon Loic.Petit.De.La.Villeon@ifremer.fr
Website: http://www.ifremer.fr/sismer/program/gsdc/homepage.htm
Responsibilities: The Upper Ocean Thermal (UOT) Data Assembly Centres (DACs) are a distributed body with several components working in partnership with the IOC/WMO sponsored Global Temperature Salinity Profile Program (GTSPP). The job of assembling the data sent either over the Global Telecommunications System (GTS) or coming in delayed mode is the task for Canada's Marine Environmental Data Service (MEDS), IFREMER of France, and the U.S. National Oceanographic Data Center (NODC). Three science centres, the Joint Australian Facility for Ocean Observation System (JAFOOS) in Australia (responsible for Indian Ocean data), Atlantic Oceanographic and Meteorological Laboratory (AOML) of the US National Oceanographic and Atmospheric Administration (responsible for Atlantic Ocean data) and Scripps Institute of Oceanographic (responsible for Pacific Ocean data) in the US carry out scientific quality assessment of the data and return their results to the main archive at the NODC.

CLIVAR Data Policy

Introduction

CLIVAR, a global multidisciplinary climate research project, requires a wide range of data and needs data centres to ingest, quality control, archive and distribute these data. The CLIVAR data policy provides guidelines for how these data should be handled in a consistent manner so as to achieve the project's scientific objectives. The policy aims to strike a balance between the rights of investigators and the need for widespread access through the free and unrestricted sharing and exchange of CLIVAR data and metadata. CLIVAR data policy is intended to be fully compatible with IOC [1], WMO [2], GCOS [3] and GEOSS [4] data principles.

The multidisciplinary nature of CLIVAR and its subprogrammes means that the principles enshrined in the data policy must be applied to data in each subprogramme's implementation plan.

Definitions used in the CLIVAR Data Policy

1. CLIVAR data

"CLIVAR data" consists of directly observed data, derived data, gridded fields, and other data products generated and/or used within CLIVAR to further its scientific goals. CLIVAR data and related products can be categorized in terms of those that are specifically sponsored or endorsed by the international CLIVAR programme, those generated by other related bodies and programmes such as the World Weather Watch of the WMO, GCOS, JCOMM, and other projects of the WCRP and those generated by relevant national and institutional CLIVAR-related projects and programmes. CLIVAR should strive to ensure that all data

relevant to CLIVAR are accessible freely and without restriction, including those collected by other projects and programmes.

2. Metadata

Metadata is defined as the descriptive information such as content, quality, condition that characterizes a set of measurements.

CLIVAR Data Policy and Principles

For CLIVAR to succeed, high-quality data and metadata need to be collected, processed and exchanged without significant delay in a free and unrestricted manner. This was recognized in the CLIVAR Implementation Plan [5] in discussing 'The Principles for CLIVAR Data'. CLIVAR data policy is enshrined in the CLIVAR data principles below:

1. Free and unrestricted exchange

All CLIVAR data should be made available freely and without restriction. "Freely" means at no more than the cost of reproduction and delivery, without charge for the data itself. "Without restriction" means without discrimination against, for example, individuals, research groups, or nationality. In exceptional circumstances involving highly specialized or experimental data, principal investigators may temporarily limit access until such time as the data can be adequately validated.

2. Timely exchanges

CLIVAR investigators should make data available voluntarily and with minimal delay, preferably also in real-time, to maximize their value to CLIVAR. In cases where extensive post-processing of delayed mode data is needed before a final research quality data set can be generated, early release of a preliminary version of the data is required.

3. Quality Control

CLIVAR investigators retain the primary responsibility for the quality of the data they produce and distribute. Data originators and those generating climate data products are required to ensure that their data meet international quality standards wherever possible.

4. Metadata

Metadata are required to enable the use of data without ambiguity or uncertainty. Metadata for CLIVAR data sets will be developed and managed in accordance with international standards.

5. Preservation of data

Long-term survival, integrity, and access to CLIVAR data must be preserved for future generations. Internationally agreed standards should be used for the acquisition, processing, and final archival of data and metadata. Data distributed in real and near-real time should, wherever possible, be replaced in a delayed mode after it has undergone quality control and full documentation.

6. Plan for re-use in reanalysis

While datasets will be used individually and in combination for research purposes, the sum total of all CLIVAR and CLIVAR-relevant data will have great value in reanalysis activities. To aid this, uniformity of data format and quality should be a high priority.

7. Easy access

CLIVAR encourages the use of the most recent advances in communication to ensure widespread access to data collected under auspices of the programme.

8. Use of existing national and international mechanisms and centres

Where feasible, CLIVAR will use existing national and international mechanisms for the exchange and storage of oceanic and atmospheric data, and build on the data management structure of existing programmes. In this way, the effectiveness of the data system will be improved by reducing redundancy and duplication and identifying opportunities and system economies, with financial costs minimized.

9. Reporting requirements

Data and metadata should be submitted to recognized data assembly centers as well as to appropriate national and international archival institutions so that the collected information may be safeguarded for future analysis. Inventories of data and related information should be readily accessible and updated as needed on a routine basis.

References

[1] IOC Data Policy (http://ioc3.unesco.org/iode/contents.php?id=200)

[2] WMO Resolution 40 (Cg-XII; see http://www.nws.noaa.gov/im/wmor40.htm)

[3] Implementation plan for the Global Observing System for Climate in support of the UNFCCC, 2004; GCOS – 92, WMO/TD No.1219.

[4] Global Earth Observation System of Systems GEOSS

10-Year Implementation Plan Reference Document (Final Draft) 2005. GEO 204. February 2005.

[5] CLIVAR Initial Implementation Plan, 1998; WCRP No. 103, WMO/TS No. 869, ICPO No. 14. June 1998.

The Workshop on Enhancing South and Central Asian Climate Monitoring and Indices, Pune, India, February 14–19, 2005

Thomas C. Peterson, National Climatic Data Center/NOAA, Asheville, NC, USA
Corresponding author: Thomas.C.Peterson@noaa.gov

The last in a series of five regional climate change workshops coordinated by the joint WMO Commission for Climatology / CLIVAR Expert Team on Climate Change Detection, Monitoring and Indices (ETCCDMI) was held in Pune, India, February 14-19, 2005. Rupa Kumar Kolli and all the people at the Indian Institute of Tropical Meteorology (IITM) did an absolutely wonderful job of hosting the workshop. My workshop teammates Phil Jones (CRU/University of East Anglia), Albert Klein-Tank (KNMI) and Mark New (Oxford University) really put their hearts into the workshop, which inspired the participants to respond in kind.

A workshop "recipe" was developed and refined during this last year. Day one started with seminars that explain how the workshop will contribute to our understanding of climate change in the region, followed by national reports from Mongolia, Kazakhstan, Tajikistan, Uzbekistan, Nepal, Bhutan, Bangladesh, Sri Lanka, Pakistan, Turkmenistan, China and the Kyrgyz Republic and India. Afghanistan was invited but the participant couldn't make it out of Kabul after a passenger plane crashed in Afghanistan the week before the meeting. Day two was devoted to Quality Control (QC) with both seminars and hands-on QC of the long-term daily data that the participants brought with them, using special software written by Xuebin Zhang (Environment Canada). A suite of 27 indices was calculated on day three, along with continuing work on QC. Day four is dedicated to homogeneity testing.

On day five, an agreement was reached on who will write the multi-authored papers documenting the changes in extremes in the region and availability of information. Participants also prepared reports showing how extremes are changing in their countries. At the workshop in Pune, all 13 countries agreed to provide their indices, the QC details they documented during their work and the homogeneity test results for a journal article and for Lisa Alexander's (Hadley Centre) global indices paper. Ten of the countries agreed to release their indices on Xuebin Zhang's ETCCDMI indices web page. Ten countries also agreed to let the lead author keep their data so he can double check the results as necessary. One country, Sri Lanka, provided its now carefully QC'd GCOS Surface Network (GSN) data from 1869 through to 2004, to put in the GSN archive. The workshop ended at lunch on day six after reports of results from each country were given and certificates of recognition were presented to each of the participants.

The Pune workshop, like three of its predecessors, was funded through GCOS by the U.S. State Department in support of IPCC. Albert Klein-Tank volunteered to be lead author of the journal paper. He will write up the analysis, carefully evaluate each station's QC, homogeneity and indices, and pass the indices on to Lisa, all before the IPCC's deadline. Also, Rupa Kumar Kolli volunteered to coordinate a monsoon season regional extremes paper with Pakistan, Sri Lanka, Bangladesh, and Nepal (Bhutan's data were too short). Xuben Zhang graciously agreed to add two new monsoon specific indices to the software to aid the analysis.

This was a workshop that involved serious hands-on data analysis work. Combined with the results of the earlier workshops in South Africa, Brazil, Guatemala and Turkey (see Figure 1), IPCC will now be able to include analysis of changes in extremes from most of the regions of the world where no results were previously available. For many countries which are unwilling to release time series of daily station data, a suite of climate change indices are being made available for use by scientists working on climate change detection or impacts. These accomplishments would not have been possible without a collaborative, capacity-building approach and the contributions by many people in GCOS, IPCC, WMO Commission for Climatology and CLIVAR who are too numerous to thank individually here. For more information on these workshops see http://cccma.seos.uvic.ca/ETCCDMI.

Figure 1: Earlier workshops were held in South Africa, Brazil, Guatemala and Turkey

Report on Tropical Atlantic workshop, 7–9th of June 2004, De Bilt The Netherlands

W. Hazeleger, Royal Netherlands Meteorological Institute (KNMI), The Netherlands
Corresponding author: hazelege@knmi.nl

Introduction

ECMWF's seasonal forecast system predicted a large chance of a shift in the position of the Atlantic Ocean's Intertropical Convergence Zone (ITCZ) for the boreal summer of 2004. However, the accuracy of this prediction was questionable because of the lack of skill of seasonal predictions with dynamical models in the tropical Atlantic. Major errors in the coupled ocean/atmosphere models are the main reasons for the lack of skill and provide compelling arguments for additional research on tropical Atlantic circulation. In June 2004, about 25 specialists on tropical Atlantic circulation met at KNMI in de Bilt (The Netherlands) to discuss recent advances in observing and modelling the tropical Atlantic and to coordinate future plans. These plans include the Tropical Atlantic Climate Experiment (TACE) that focuses on improving the understanding of SST-ITCZ interactions in the eastern Tropical Atlantic region, the African Multidisciplinary Monsoon Analysis (AMMA) that focuses on the African Monsoon and it's offshore components, and the Atlantic Marine ITCZ (AMI) project.

Summary of the presentations

In the first part of the meeting much attention was directed at the western tropical Atlantic. New hydrographic data shows mounting evidence for large cross-equatorial and cross-gyre transport of Southern Hemisphere surface and thermocline waters in North Brazil current eddies and subsurface eddies. Saline water masses from the South Atlantic are observed at the passages of the Caribbean. After crossing the equator, much of the North Brazil Current transport also feeds the Equatorial Undercurrent, which carries primarily water originating from the Southern Hemisphere. Transport from the North Equatorial Current has been shown to feed both the North Equatorial Countercurrent and the North Equatorial Undercurrent. It was shown that altimeter data and new high-resolution ocean model data confirm this picture of western tropical Atlantic circulation.

The Deep Western Boundary Current and deep equatorial jets dominate deep circulation in the tropical Atlantic. The jets are probably generated by inertial instability. Surprisingly, both in the deep jets and in the Deep Western Boundary Current strong variability is found. In the Deep Western Boundary Current large anticyclonic eddies have been observed along the Brazilian coast.

Satellite data show that the Bjerknes feedback mechanism that relates wind stress to thermocline depth is operating on the equator. Also, these data show intraseasonal variability signals that are not well understood yet. Slow variations in salinity in the ventilated layers are observed in hydrographic data and are probably caused by changes in ventilation rates. However, from ocean models of the Atlantic it is still unclear whether variability in atmospheric forcing and associated variations in subtropical cells can generate sizeable variability on the equator. Atmospheric connections between remote regions and the tropical Atlantic are indicated by data and need to be studied further. Coupled models show large biases, but careful tuning of mixed layer parameterizations improves the simulation of tropical Atlantic climate. Also, discrepancies in shallow atmospheric convection are found among models and reanalysis sets. Discrepancies in mixed layer climatologies are found as well. Due to the large biases, the skill of the predictions in the tropical Atlantic region is low, while there is large potential predictability of rainfall on the African and South American continent (i.e. if SST is prescribed in the models). Multi-model ensembles overcome some, but certainly not all, problems with the lack of forecast skill. Finally, climate change affects the tropical Atlantic region as well and changes in Sahel rainfall were shown in a coupled model study.

The last day of the workshop was reserved for planning and discussion on future observations and modelling. Current programs and plans for the coming years were presented: the CLIVAR – TACE initiative, the European Union funded AMMA program, the Enabling Grids for E-sciences (EGEE) and Pilot Research Moored Array in the Tropical Atlantic (PIRATA) programs, the US CLIVAR – AMI initiative and the plans of the hydrographic work by University of Bremen, NOAA/AOML and IFM/Geomar.

Discussion sessions and recommendations

The discussion sessions were directed at formulating objectives for the CLIVAR – TACE initiative and coordinating these objectives with the other programs such as AMMA and AMI. There was consensus that the eastern tropical Atlantic is important for climate variability in the tropical Atlantic region. There is a clear connection between eastern tropical Atlantic SST and ITCZ position and strength, while the processes that regulate SST are not well understood. This absence of understanding argues for additional research effort in this region. The central goal of this research would be:

Improve understanding of the interaction between the ITCZ and upwelling zones (Benguella region, Guinea dome, eastern cold tongue) and the implications for predictability.

The discussions set out with this central goal and recommendations for observations and modelling were made.

Figure 1 (page 15) shows the observations needed for TACE (constructed by W. Johns, Rosentiel School of Marine and Atmospheric Science). Several of these observations have already been proposed for AMMA for deployment in 2006 (e.g., additional PIRATA moorings and surface drifting buoys). Figure 1 summarizes the recommendations based on discussions of observational needs. This encompasses an enhanced observation period of 1 – 5 years in the eastern tropical Atlantic that aims to determine:

- Mixed layer heat budget and subsurface heat content
- Surface and subsurface current structure and their role in modulating the heat budget and thermocline properties
- Shallow and deep atmospheric circulation in the marine ITCZ complex

The recommended oceanic observations focus on a line along 23°W, which is the same line where atmospheric observations are proposed for the AMMA and AMI projects. Moorings along this line and in the upwelling regions in the Southern Hemisphere are proposed as well as glider sections with oxygen sensors to determine upwelling. Also, enhanced deployment of Argo floats and surface drifters in the region is recommended. The plans will be coordinated with the cruises in the same region planned in the French EGEE project.

The focus on mixed layer heat budget and subsurface heat content in the upwelling zones was welcomed by the modellers at the meeting. In the upwelling regions the models fail to simulate accurately upper layer conditions and validation of the simulated mixed layer and subsurface heat budget by observations is thought to be essential for progress. The modelling studies that are needed aim to:

- Improve SST forecasts in the tropical Atlantic region (seasonal to interannual)
- Determine the response of tropical Atlantic region to global warming

It was recommended that the main focus of ocean model improvement needs to be on diapycnal oceanic mixing and mixed layer physics. Atmospheric modelers need to focus on stratus clouds/radiation feedbacks and shallow and deep convection. Specific projects that were proposed include a systematic investigation of the impact of ocean model resolution and of the impact of ocean/atmosphere coupling on the simulation of sea surface temperature in the tropical Atlantic region. Also, studies on potential predictability with atmospheric models and studies on the effect of dust were recommended.

The workshop made clear that the emphasis of future work will be on the eastern tropical Atlantic. With a wealth of data available from the western tropical Atlantic it is now the appropriate time for synthesis activities on the western tropical Atlantic. R. Molinari (NOAA/AOML) will coordinate these activities.

The stimulating annual tropical Atlantic meetings will be continued. P. Rizzoli (MIT) will organize a follow up, tentatively scheduled for October 2005 in Venice. The program, a list of participants, and most presentations of the meeting at KNMI can be found online at: http://www.knmi.nl/samenw/tameet/tameet.html

Challenges in Prediction of Summer Monsoon Rainfall: Inadequacy of the Two-Tier strategy

Bin Wang[1], Xiouhua Fu[1], Qinghua Ding[1], In-Sik Kang[2], Kyung Jin[2], J. Shukla[3], and Francisco Doblas-Reyes[4]
[1]School of Ocean & Earth Science & Technology, University of Hawaii, USA
[2]School of Earth and Environmental Sciences, Seoul National University, Korea
[3]Climate Dynamics, George Mason University, USA
[4]European Centre for Medium-Range Weather Forecast, UK
Corresponding author: wangbin@hawaii.edu

The scientific basis for climate prediction lies in the predictability determined by slow variations of the ocean and land surface conditions (Charney and Shukla 1981; Shukla 1998). Based on this premise, the atmospheric general circulation models (AGCMs) are expected to be able to capture the predictable portion of the tropical rainfall if the slowly varying boundary forcing is known.

In a recent assessment of AGCM performance in simulation of Asian monsoon, Wang et al. (2004) found that the eleven AGCMs that participated in a CLIVAR-related monsoon intercomparison project show no skill in their ensemble simulations of the summer rainfall anomalies in a large region from 5°N to 25°N and from 70°E to 150°E. They speculate that neglect of air-sea interaction is a possible cause of the models' failure.

Here we show that the poor simulation of the summer monsoon rainfall found in Wang et al. (2004) is not specific to the unprecedented 1997/98 El Niño episode, rather it is a general monsoon 'syndrome' in monsoon seasonal prediction. We have recently examined the skills of five state-of-the-art AGCMs in hindcasting seasonal precipitation for a 20-year period from 1979-1998. These models were forced by identical observed SST and sea-ice - a procedure that follows the design of the Atmospheric Model Intercomparison Project (AMIP) (Gates et al. 1999). Each model made 6 to 10 integrations in order to reduce the "noise" due to atmospheric internal dynamics. The multi-model ensemble (MME) sums up all models' ensemble means to further reduce the uncertainties associated with the models' physical parameterization of sub-grid scale processes such as cumulus convection.

Figure 1 (page 15) shows the overall skill of the five-model ensemble hindcast. While all models have high skills in the El Niño region (10°S-5°N, 160°E-80°W), on average these models and their MME have virtually no skill in the Asian-Pacific summer monsoon (APSM) region (5°N-30°N, 70-150°E). A fundamental question needs to addressed is why nearly all AGCMs, when they are given the observed lower-boundary forcing, unable to forecast the summer monsoon precipitation anomalies?

A key to seasonal prediction is to understand the relationship between the slowly varying boundary conditions and rainfall anomalies. We found that all models tend to yield positive SST-rainfall correlations in the heavily precipitating summer monsoon regions that are at odds with observations. As shown in Fig. 2a (page 16), the local SST and precipitation anomalies are negatively correlated in the western North Pacific (WNP, 5°N-30°N, 110-150°E) and insignificantly correlated in the Bay of Bengal. However, the SST-rainfall correlations in the MME hindcast disagree with observations primarily in the APSM regions, where the model rainfall tends to correlate positively with local SST (Fig. 2b page 16). Over the WNP, the observed correlation is –0.36 while in the multi-model ensemble hindcast it is 0.24, both statistically significant at the 99% confidence level. The models' inability to predict summer monsoon rainfall appears to happen because the models produce a wrong relationship between rainfall and SST in that region.

In general, a negative correlation between the seasonal-mean SST and rainfall anomalies may indicate that the atmosphere, on average, affects SST more than SST affects the atmosphere; conversely, a positive correlation means that the ocean plays a major role in determining the atmospheric response (Wang et al. 2004). To support this assertion, we further computed the lag correlations between monthly mean SST and rainfall anomalies. As shown in Fig. 3a (page 16), when precipitation leads SST by one month, there is a significant negative relation in the APSM region, suggesting that the atmosphere influences SST variability. Of note is that the simultaneously monthly correlations are also negative though in less degree. However, when SST precedes precipitation by one month, the correlations in the same region become positive. Given the persistence of SST anomalies and the rapid response of the atmosphere to SST, the negative simultaneous correlation and the weak positive lag correlation suggest that the impact of SST on the atmosphere is weak. Thus, the SST anomalies in the APSM region cannot be interpreted as a forcing; rather the SST anomalies in this region are, on an average, determined by the anomalous atmospheric conditions.

The finding that the models are unable to reproduce the observed SST-rainfall relationship provides a clue to why these models are unsuccessful in hindcasting summer monsoon rainfall. While the models' deficiencies are somewhat to blame, we offer that the models' failures are likely due to the lack of atmospheric feedback to the ocean, an inherent problem in the experimental design, because in the hindcast experiments the SST is prescribed as a forcing.

To test this idea, we performed a suite of numerical experiments with a coupled atmosphere-ocean model. The atmospheric component of this coupled model is the T30 version of the ECMWF-Hamburg (ECHAM4) AGCM (Roeckner et al. 1996). The ocean component is a 2-layer tropical upper-ocean model (Wang et al., 1995; Fu and Wang, 2001). The coupling, namely atmosphere-ocean interaction, was through both the momentum and heat flux exchanges without flux correction. Daily coupling was applied to the global tropics between 30°S and 30°N and climatological SSTs outside the tropics and sea ice were specified. The coupled model was integrated for 50 years, and the last 40 years of data were used for analysis. This coupled model, in general, realistically simulates the climatological mean precipitation and SST, the spatial pattern and temporal characteristics of El Niño-Southern Oscillation, and the tropical intraseasonal oscillation (Fu et al. 2003). In the coupled experiment, the AGCM is allowed to interact with a tropical ocean model. For comparison a "forced" experiment was also performed in which the same AGCM was integrated using, as lower boundary forcing, the same SSTs that were produced by the coupled model. The only difference between the coupled and forced experiments is in their initial conditions, which are trivial for climate simulation and prediction. The differences in the simulation outcomes between the two experiments can be interpreted as being due to the lack of atmospheric feedback.

Figure 3b (page 16) presents the results obtained from the coupled model simulation. The simultaneous and the lag correlation patterns bear qualitative similarities with the corresponding observed counterparts, although in the coupled simulation the simultaneous negative correlations are somewhat lower and the positive correlations at lag +1 are higher. When rainfall leads SST by 1-month, the monsoon precipitation and SST are significantly negatively correlated, resembling closely the observations. In contrast, the results obtained from the forced experiment (Fig. 3c) show a significant concurrent positive correlation and similar positive, but lower, lead-lag correlations. This persistent positive correlation pattern with a concurrent maximum suggests that the slow variations of SST in the model act to regulate local rainfall anomalies. The atmospheric response to the underlying SST forcing is sufficiently rapid to cause the maximum monthly correlation to occur without a lag.

The coupled model results have been compared with the newly released multi-model seasonal prediction experimental results from the European Union-funded DEMETER project (*D*evelopment of a *E*uropean *M*ulti-model *E*nsemble system for seasonal to in*ter*annual prediction) (Palmer et al. 2004). The coupled model forecasts for boreal summer (May to October) demonstrate that the local SST-precipitation relationships in all the models are similar to that shown in Fig. 3b, confirming that these coupled models, despite their different physical schemes, are able to produce qualitatively realistic SST-rainfall relationships. In addition, when these atmospheric models are driven by persistent SSTs the local SST-rainfall correlations become similar to those found in the forced run (Fig. 3c).

In summary, we have demonstrated that coupled atmosphere-ocean models can reproduce realistically the lead/lag correlation between SST and precipitation anomalies. However, if the same atmospheric model is forced by the SST anomalies that are produced by the coupled model, the resulting local SST-rainfall relationships are at odds with observations, similar to those that participate in multi-model ensemble hindcasts. In reality and in the coupled model, the SST in the warm pool is primarily a result of atmospheric forcing, thus, the abnormal precipitation and SST are negatively correlated. On the other hand, if the SST is considered as a forcing to the model atmosphere (the AMIP design or tier-two system design) the atmospheric model is unable to reproduce the correct rainfall anomalies, because the forced

response tends to produce a positive local rainfall-SST relationship.

The present finding suggests that contrary to conventional notion, the heavy summer monsoon rainfall cannot be simulated or predicted correctly by prescribing lower boundary forcing. The coupled atmosphere-ocean processes are extremely important for seasonal prediction of monsoon rainfall. This calls for rethinking current strategies for validating dynamic climate models and for climate prediction. To adequately identify the deficiencies of models in simulating summer monsoon variability, a coupled atmosphere-ocean model is needed. The current two-tier approach predicts future atmospheric conditions using an AGCM alone forced by pre-forecast SSTs (Bengtsson et al. 1993). This strategy works for the most important forcing (Equatorial Pacific SST forced heating) and for those regions where SST determines the local wind convergence and SST itself is primarily determined by ocean processes. However, in the Asian-Pacific summer monsoon regions, where atmospheric feedback plays a major role in determining local SST, the two-tier approach would yield a forced solution that differs from realistic coupled solutions. Therefore, only coupled atmosphere-ocean models or regionally coupled models will be able to correctly forecast the predictable portion of the monsoon rainfall. Further studies of the climate predictability in the summer monsoon regions using more models and longer term integrations are needed to confirm that the present conclusions are independent of models' physical parameterizations.

Acknowledgments

This work is in part supported by NSF Climate Dynamics program and NOAA OGP/Pacific Program. DR was supported by the EU-funded DEMETER project (EVK2-1999-00024).

References

Bengtsson, L., U. Schlese, E. Roeckner, M. Latif, T. Barnett, and N. Graham, 1993: A two-tiered approach to long-range climate forecasting. *Science*, **261**, 1026-1029.

Charney, J. G., and J. Shukla, 1981: Predictability of monsoons. *Monsoon Dynamics*, J. Lighthill and R. P. Pearce, Eds., Cambridge University Press, 99-109.

Fu, X., and B. Wang, 2001: A coupled modeling study of the seasonal cycle of the Pacific cold tongue. Part I: simulation and sensitivity experiments. *J. Climate*, **14**, 765-779.

Fu, X., B. Wang, T. Li, and J. P. McCreary, 2003: Coupling between northward-propagating, intraseasonal oscillations and sea-surface temperature in the Indian Ocean. *J. Atmos. Sci.*, **60**, 1733-1753.

Gadgil, S., and S. Sajani, 1998: Monsoon precipitation in the AMIP runs. *Climate Dyn.*, **14**, 659-689.

Gates, W. L., and coauthors, 1999: An overview of the results of the Atmospheric Model Intercomparison Project (AMIP I). *Bull. Amer. Meteor. Soc.*, **80**, 29-56.

Palmer, T. N., and coauthors, 2004: Development of a European multi-model ensemble system for seasonal to inter-annual prediction (DEMETER). *Bull. Amer. Meteor. Soc.*, in press.

Reynolds, R. W., N. A. Rayner, T. M. Smith, D. C. Stokes, and W. Wang, 2002: An improved in situ and satellite SST analysis for climate. *J. Climate*, **15**, 1609-1625.

Roeckner, E., and coauthors, 1996: The atmospheric general circulation model ECHAM-4: model description and simulation of present-day climate. Max-Planck-Institute for Meteorology, Rep.218, 90 pp.

Shukla, J., 1998: Predictability in the Midst of Chaos: A scientific basis for climate forecasting. *Science*, **282**, 728-731.

Wang, B., T. Li, and P. Chang, 1995: An intermediate model of the tropical Pacific Ocean. *J. Phys. Oceanogr.*, **25**, 1599-1616.

Wang, B., I. S. Kang, and J. Y. Lee, 2004: Ensemble simulations of Asian-Australian monsoon variability by 11 AGCMs. *J. Climate*, **17**, 803-818.

Xie, P., and P. A. Arkin, 1997: Global precipitation: A 17-year monthly analysis based on gauge observation, satellite estimates, and numerical model outputs. *Bull. Amer. Meteor. Soc.*, **78**, 2539-2558

WCRP is celebrating its 25th anniversary and, as a first way to mark the event, has published a new WCRP Brochure

The publications is available on the website news page: http://www.wmo.ch/web/wcrp/news.htm

Seasonal and annual predictions of sea surface temperature anomalies over the tropical Pacific Ocean by using a multi-models system

Zong-Ci Zhao, Zuqiang Zhang and Qingquan Li
National Climate Center, China Meteorological Administration, Beijing, China
Corresponding author: zhaozc@cma.gov.cn

Abstract

A multi-model system has been used to predict the seasonal and annual sea surface temperature anomalies (SSTA) over the tropical Pacific Ocean since 1997 in the National Climate Center (China). The evaluations of the multi-model system indicated that the ensemble multi-model predictions were better than those using by a single model.

Introduction

Many Chinese researchers have pointed out the significant correlations between the SSTA over the ENSO regions, Kuroshio and the warm pool areas of the tropical Pacific Ocean and the summer rainfall in China, as well as typhoons over the northwestern Pacific Ocean (Wang, 2001). Therefore, it is important to forecast the SSTA over the tropical Pacific Ocean.

A project on the use of a multi-model system for seasonal and annual forecasts of the SSTA over the tropical Pacific Ocean was conducted in China during the period 1996 to 2000. Several modelling groups such as the National Climate Center (NCC, China), Chinese Academy of Meteorological Sciences (CAMS), Peking University (PKU), Nanjing University (NJU), Nanjing Institute of Meteorology (NIM) and Institute of Shanghai Typhoon (STI) took part into this project (Zhao et al., 2001). Since the beginning of 1997, the multi-model system joined the National Workshops on multi-seasonal predictions in China held by the China Meteorological Administration and Hydrological Department.

In this paper, a brief description of the multi-model system and its predictions will be introduced.

Brief description of the multi-model system

There are five models in the multi-model system (Li et al., 2000; Zhao et al., 2001). They are the NCCo based on Zebiak and Cane (1987, ZC87) with improved initial conditions (Li and Zhao, 2001), NCCn based on ZC87 with improvements to some parameters in the model (Zhang and Zhao, 2000), CAMS/NJU based on ZC87 and developed for the global tropical Ocean (Atlantic, Indian and Pacific Oceans) (Ni et al., 2000; Shi et al., 2000), STI/NCC based on ZC87 but with assimilation of inputs as in Duan et al., 2000; Liang et al., 2000, and NIM/NCC based on the Oxford model (Balmaseda et al, 1994) with improvements to the statistical atmosphere and some parameters in the ocean model (Zhang and Ding, 2000).

In the multi-seasonal predictions by the multi-model system, each model was first run to produce an ensemble size of 5 or 6; secondly, the ensemble of the five sets of model predictions was taken as the multi-model system's predictions. Because the National Workshop is held in March of each year, the multi-model system predicted the period of the coming March to the following February. The system predicted the monthly SSTA over the tropical Pacific Ocean and in NINO regions (such as Nino1+2, Nino3, Nino3.4 and Nino4). The multi-model system also provided the predictions of SSTA (October ~ next September and June ~ next May) in the Annual Workshop held in October and the Special Summer Workshop of China held in June, respectively.

The seasonal and annual hindcasts and prediction of Nino3 index by the multi-model system have been evaluated for the periods of 1961~1996, 1997~2000 and 2001~2004 using anomalous correlation coefficients and standard deviations, respectively (Li et al., 2000; Zhao et al., 2000; Zhang, 2004).

Predictions

The evaluations of the seasonal and annual hindcasts of Nino3 index by the multi-model system indicated that the ensemble multi-model were better than a single model. For 1997~2004, the multi-models system predicted the weakening of El Nino events reasonably, but the starting time of El Nino events was unstable. As two examples from 2000~2004, Fig.1 and Fig.2 (page 17) give the predictions of Nino3 index for March 2001 ~ January 2002 predicted by February 2001 and for October 2003 ~ September 2004 predicted by September 2003, respectively.

Future

The multi-model system for the seasonal and annual predictions of SSTA was made up of the simplified models. The system is going to be improved in future. The predictions of SSTA by the coupled AOGCM of NCC will be combined with the system.

Acknowledgements

This research was supported by the National Key Projects and extension project of China. We sincerely thank M.Cane and S.Zebiak and National Climate Center (China) for their guidance and support.

References

Balmaseda, M. A., D. L. T. Anderson and M. K. Davey, 1994: ENSO prediction using a dynamical ocean model coupled to statistical atmospheres. *Tellus*, 46A, 497-511.

Duan, Y and Liang X, 2000, Investigation of STI/NCC, *Acta Meteorologica Sinica*, 870-880 (in Chinese).

Li, Q, Zhao Z-c, Zhang Z, Yi L, Zhang Q, Liang X, Duan Y, Li Y, Shi L, Yin Y, Ni Y, 2000, The predictions of the 1997~1999 El Nino/La Nina events by using an intermediate ocean-atmosphere coupled model system, *Acta Meteorologica Sinica*, 838-847 (in Chinese).

Li Q and Zhao Z-c, 2001, Diagnostic analysis and verification of prediction of the tropical Pacific Sea surface temperature anomalies during 1997~1998, *J.of Tropical Meteorology*, 7, 144-153.

Li, Q, 2001, Prediction of SSTA for 2001, report at National Workshop of 2001 (in Chinese).

Liang X and Duan Y, 2000, Predictions of ENSO by STI/NCC, *Acta Meteorologica Sinica*, 891-897 (in Chinese)

Ni, Y, Li S and Yonghong Y, 2000, Investigation of CAMS/NJU, Acta Meteorologica Sinica, 848-858 (in Chinese).

Shi, L, Yongqi N and Yin Y, 2000, Experiments of SSTA predictions over the global tropical oceans, *Acta Meteorologica Sinica*, 859-869 (in Chinese).

Wang, S-W, ed, 2001, Advances on modern climatology, China Meteorological Press, Beijing, China, pp450 (in Chinese).

Zebiak,S.E. and Cane,M.A.,1987:A model of the El Nino-Southern Oscillation. *Mon.Wea.Rev.*115,2262-2278.

Zhang, Q and Yihui D, 2000, Investigation on NIM/NCC model and its prediction, Acta Meteorologica Sinica, 880-890 (in Chinese).

Zhang Z and Zhao Z-c, 2000, The simplified ENSO prediction model NCCn, Short-term Climate Prediction Operation Dynamic Model, ed. By 96-908 Project, China Meteorological Press, 351-361 (in Chinese).

Zhang, Z, 2003, Annual predictions of SSTA, report at National Workshop of 2003 (in Chinese).

Zhang, Z, 2004, Perfomance of the NCC multi-models system for the prediction of SSTA, Report of NCC (in Chinese).

Zhao, Z-c, Qingquan L, Zuqiang Z, Lan Y and Zongqun Z, 2000, Relationships between ENSO and climate change in China and predictions of ENSO, *World Resource Review* (USA), **12**, 2, 269-279.

Zhao Z-c, Li Q, Zhang Z, Yi L, Zhang Q, Liang X, Duan Y, Li Y, Shi L, Yin Y, Ni Y,, Qian W, Li L, and Sun Y, 2001, Advances on a dynamic prediction model system of ENSO, Short-term climate prediction dynamic model system, ed. By 96-908, China Meteorological Press, 323-335 (in Chinese).

Predictability of the March precipitation in the Mediterraneo–Atlantic region by the PNA pattern

C. Norrant and A. Douguédroit
Institute of Geography, University of Provence, France
Corresponding author: caroline.norrant@up.univ-aix.fr

A significant decrease of rainfall has been detected during March in the second half of the 20th century in Spain and Portugal (Trigo and DaCamara, 2000) and in the whole Mediterranean-Atlantic region (Norrant and Douguédroit, 2004). A link between Pacific atmospheric circulation indices, particularly ENSO, and springtime precipitation in Spain has been detected (Rodo et al., 1997, Knippertz et al., 2003). Our research looks for the low frequency circulation patterns of the northern hemisphere that can influence the March precipitation decrease in the Mediterranean-Atlantic region from 1951 to 2000. The relationship was studied simultaneously and with a one and two month lead time, to take into account the delay necessity for the Rossby waves to propagate from the Pacific to the western Mediterranean (Benedict et al., 2004).

1. Data and methods

Scores linked with the factor of a Rotated Principal Component Analysis (RPCA), of R type and with a Varimax rotation (Richman, 1986), on 61 stations of the Mediterranean Basin and the Atlantic coast at the same latitude from March 1951 to March 2000, form the precipitation data.

The 500hPa geopotential height data (March, February and January) come from the NCEP/NCAR reanalysis project; a window of the northern hemisphere north of 20°N has been retained, with a diamond grid similar to that of Barnston and Livezey (1987). The main hemispheric teleconnection indices (NCEP/NCAR) have also been used.

RPCAs, R type, have been performed on the March, February and January 500hPa geopotential heights in order to detect the main low frequency patterns of the atmospheric circulation.

2. Results

2.1. RPCA on the 500hPa geopotential height

In the 12 retained factors (79,7% of the total variance) of the RPCA on the March 500hPa geopotential height, four patterns are significantly correlated with the Mediterranean-Atlantic region rainfall and explain 36% of their total variance. Two of them fit the EAtl/WRussia and NAO patterns spatial schemes (Barnston and Livezey, 1987) (Figure1, Table 1).

Among the fifteen factors retained from the RPCA on the February 500hPa geopotential height, 3 significantly correlated with the Mediterranean-Atlantic region only represent 16% of the total variance. For January they are, among a total of thirteen, 3 with 33% of explained variance (Figure 2, Table2). The strong negative correlation with the January PNA which explains on its own nearly 25% of the March rainfall in the Mediterranean-Atlantic region can be highlighted.

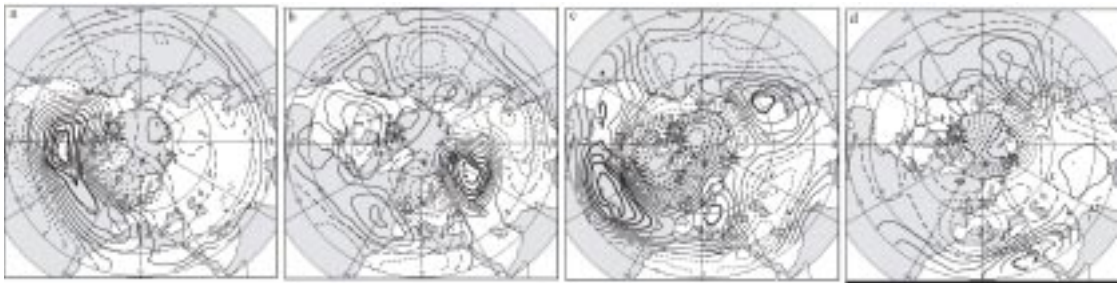

Fig.1: March patterns significantly correlated with the March rainfall of the Mediterraneo-Atlantic region. Solid line: positive correlation; dashed line: negative correlation; bold: correlation ≥0,5; contour increment: 0,1

	EAtl	EAtl/WRussia	EPac	NAO	PNA	Scan	WPac	AO	SOI
March	-.11	**.25**	-.19	**-.45**	**-.29**	.13	**-.23**	**-.34**	.18
Feb	**-.36**	.05	-.03	-.13	-.01	.13	-.03	-.19	.10
Jan	**-.28**	-.09	-.07	.12	**-.49**	**-.20**	**-.29**	.06	.19

Tab.1: Correlation of March rainfall in the Mediterraneo-Atlantic region with the main hemispheric teleconnection indices. Significant correlations are in bold.

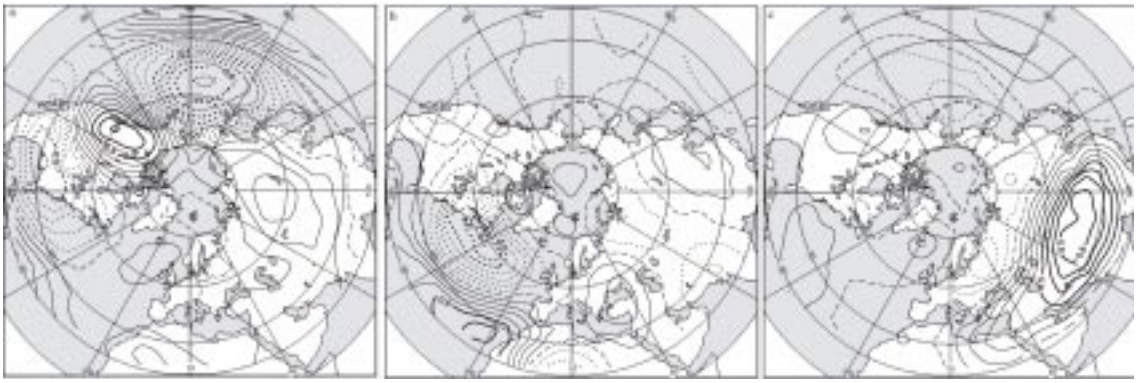

Fig.2: January patterns significantly correlated with March rainfall of the Mediterraneo-Atlantic region. Solid line: positive correlation; dashed line: negative correlation; bold: correlation ≥0,5; contour increment: 0,1

Patterns	Eastern Canada	EAtl / WRussia	NAO	Northern Siberia	PNA	EAtl	Eurasia
March	-.36	.32	-.39	.20	-	-	-
January	-	-	-	-	-.44	-.30	-.21

Tab. 2 Significant correlation between the scores of the March and January 500hPa geopotential height patterns and the March rainfall of the Mediterraneo-Atlantic region.

2.2. Correlation with the main hemispheric teleconnection indices

The correlation give the same results as the RPCA but new teleconnections with significant but weak correlation are discovered (WPac, AO) (Table 1). With a one month lead time, the single EAtl index is significantly correlated. With a two months leading time the teleconnections with the PNA index are found again. March rainfall in the Mediterranean-Atlantic region is explained at 25% by the PNA, which is the only pattern representing an important variance in the analysis.

3. Conclusion

36-40% only of the March rainfall in the Mediterranean-Atlantic region is explained by correlation with March RPCA patterns and teleconnection indices. A significant result has been obtained for their prediction with a two months lead time: PNA pattern explains 25% of their total variance. It seems to confirm the relationship previously established between Pacific and spring precipitation in western Europe by the ENSO index at a seasonal leading time (Rodo et al., 1997, Knippertz et al., 2003).

References

Barnston AG, Livezey RE, 1987: Classification, seasonality and persistence of low frequency atmospheric circulation patterns, *Monthly Weather Review*, **115**: 1825-1850

Benedict JJ, Lee S, Feldstein SB, 2004 : Synoptic view of the North Atlantic Oscillation, *J. Atm. Sc.*, **61**: 121-144

Knippertz P, Ulbricht U, Marques F, Corte-Real J, 2003 : Decadal changes in the link between El Niño and springtime North Atlantic Oscillation and European-North African rainfall, *Int. J. Climatol.*, **23**: 1293-1311

Norrant C; Douguédroit A, 2004 : Monthly and daily precipitation trends in the Mediterranean (1950-2000), *Theor. Appl. Climatol.*, submitted

Richman MB, 1986: Rotation of principal component, *J. Climatol.*, **6**: 293-335

Rodo X, Baert E, Comin FA, 1997 : Variations in seasonal rainfall in Southern Europe during the present century : relationships with the North Atlantic Oscillation and El Niño – Southern Oscilation, *Climate Dynamics*, **13** : 275-285

Trigo RM, DaCamara CC, 2000: Circulation weather types and their influence on the precipitation regime in Portugal, *Int. J. Climatol.*, **20**: 1559-1581

Skill of Sahelian rainfall index in two atmospheric General Circulation model ensembles forced by prescribed sea surface temperatures

Vincent Moron
International Research Institute for Climate Prediction, Columbia University, Palisades, USA
Corresponding author: vincent@iri.columbia.edu

Introduction

Sea surface temperatures (SST) changes have long been recognized as a forcing mechanism for rainfall variations in the West-African monsoon area (e.g. Rowell *et al.*, 1995; Ward, 1998; Thiaw *et al.*, 1999). For example, anomalous negative (positive) rainfall anomalies over the Sahelian belt (approximately between 10° and 20°N across tropical North Africa) have been associated with positive (negative) SST anomalies (SSTA) throughout almost much of Indian Ocean, South and equatorial Atlantic, negative (positive) SSTA over the tropical Northern Atlantic and warm (cold) El Niño Southern Oscillation events (e.g. Rowell *et al.*, 1995 ; Ward, 1998). SST forcing is thus potentially able to provide predictability to the Sahelian belt at seasonal time scales. Hindcast (i.e. forecast for past periods) ensembles are a standard method of estimating the uncertainty in seasonal climate prediction by sampling the distribution of possible outcomes conditional upon a given SST pattern. The potential predictability (estimated through the degree of similarity amongst an ensemble of runs that differ only by their initial conditions) and skill (estimated through the similarity between simulated and observed variability) could be based on atmospheric general circulation model (AGCM) simulation using observed SST (Sperber and Palmer, 1996). These AGCM simulations provide an indication of model performance assuming perfect SST forecasts. There are various sources of errors, decreasing the potential predictability and skill of any simulated variable such as rainfall. The chaotic evolution of the atmosphere is one major source. Over the Sahel, the percentage of SST-forced variance in seasonal rainfall amount is typically below 25-50% (10-30%) on a regional (grid-point) basis. A large part of the inter-annual variability of the seasonal rainfall is thus unpredictable from the global SST anomalies. The simulated rainfall fields could be shifted spatially relatively to observation. There are also deficiencies due to truncation and the parametrization schemes used to generate rainfall in the AGCMs. All these errors may be model- and time scale-dependent. The skill of a Sahelian rainfall index is here investigated in two large AGCM ensembles forced by prescribed SST over the post-war II period.

Models experiments and observed data

The simulated rainfall were provided by the outputs of the ARPEGE and ECHAM 4.5 AGCMs, run respectively at the T63L30 and T42L19 resolution in a simulation mode, are used. Both ensembles (8-member for ARPEGE and 24-member for ECHAM 4.5) are forced by prescribed SST from 1948 to 1997 (ARPEGE) and from 1950 (ECHAM 4.5). These runs have been extensively presented elsewhere (Cassou and Terray, 2001; Moron *et al.*, 2003, 2004 for ARPEGE; Tippett *et al.*, 2004; Gong *et al.*, 2003 for ECHAM 4.5). The observed rainfall was obtained from the Climatic Research Unit dataset (version 1.0 ; http://www.cru.uea.ac.uk/~mikeh/datasets/global/) at the 3.75° x 2.5° resolution. Monthly data are available from 1901 to 1998 but 1997 is completely missing over the Sahel. So, the data from 1950 to 1996 are used in the following analysis. In this paper, we define the Sahel as the region between 16°W-20°E and 11.25°-18.75°N. Time series of seasonal rainfall within the sahelian box are standardized to zero mean and unit variance. The standardized anomaly index (SRI hereafter) is the mean of these values (Katz and Glantz, 1986). To ease the comparison between observation and models, SRI is then re-standardized to unit varinace. Each run of both AGCMs is processed independently from each others (i.e. data are firstly standardized on a grid-point basis, then averaged into the SRI box, and SRI is thus standardized to unit variance). In the following SRI_{obs}, SRI_{echam} and SRI_{arp} refer respectively to observed SRI, and simulated SRI with ECHAM 4.5 and ARPEGE. Some of the correlations are computed on two different time scales, following Ward (1998). The low frequency (LF hereafter) time scale is firstly extracted from the original time series using a nine order Butterworth low-pass filter with a cut-off at 1/8 cycle-per-year (i.e. retaining only periods less than 0.125 cpy). The high frequency (HF) variability is then defined as the difference between the original time series and the LF ones.

continued on page19

From Hazeleger, Page 7: Report on Tropical Atlantic Workshop

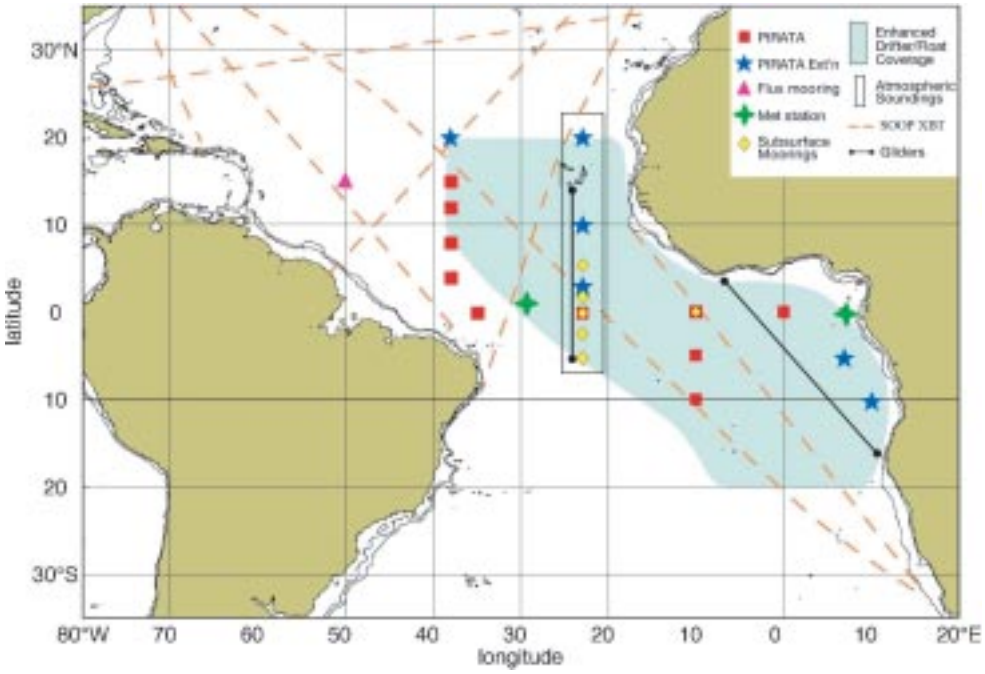

Figure 1: Scheme showing proposed observtions during the 1-5 year enhanced observation period of CLIVAR-TACE (courtesy of W. John, RSMAS)

From Wang et al Page 8: Challenges in Prediction of Summer Monsoon Rainfall: Inadequacy of the two-tier strategy.

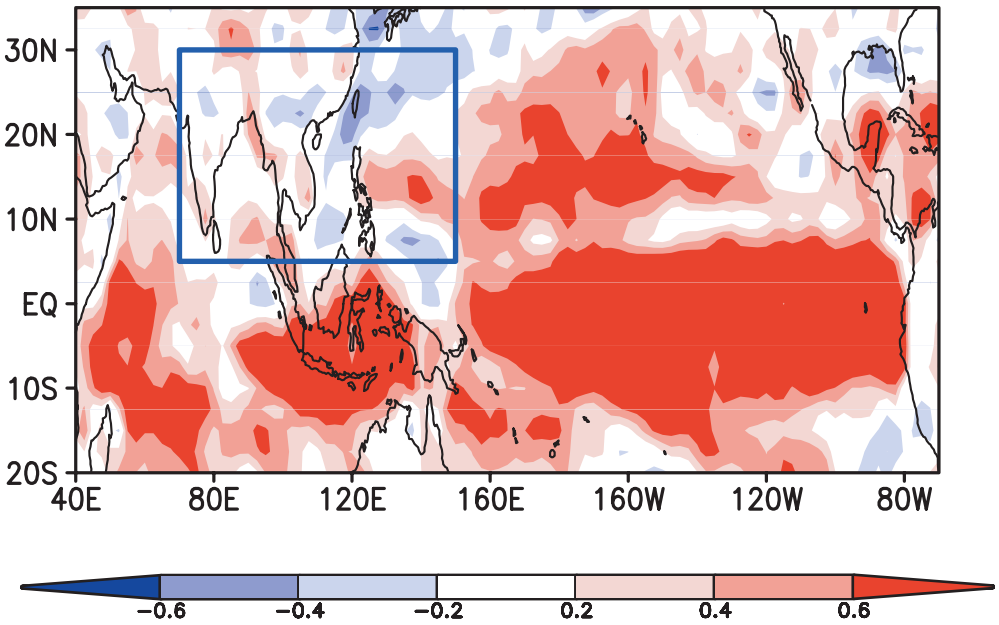

Figure 1: Correlation coefficients between the observed (Xie and Arkin 1997) and the hindcasted June-August precipitations for the period 1979-1999. The hindcast was made by five AGCMs' multi-model ensemble (MME) mean. These models are the operational seasonal prediction models from National Center for Environmental Prediction (NCEP), Japan Meteorological Agency (JMA), Center for Ocean-Land-Atmosphere (COLA), National Aeronautical Space Agency (NASA), and Seoul National University/ Korean Meteorological Administration (SNU/KMA).

From Wang et al Page 8: Challenges in Prediction of Summer Monsoon Rainfall: Inadequacy of the two-tier strategy.

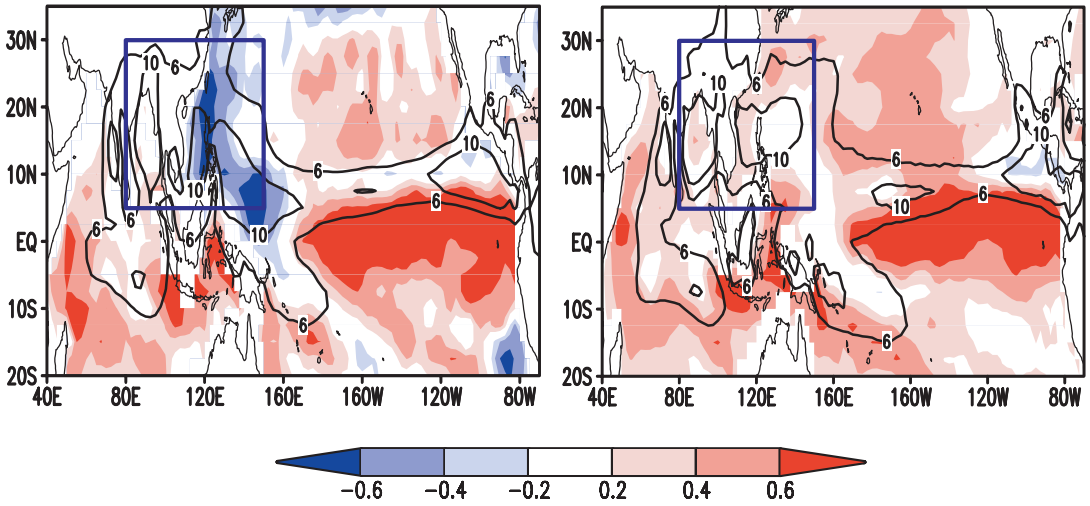

Fig. 2. (a) Observed and (b) simulated correlation coefficients between the June-August SST and precipitation anomalies (the color shadings). The contours denote the climatological June-August mean rainfall rate (in units of mm day^{-1}) that highlight the regions of heavy precipitation. The observed correlations were computed using 20 years of data (1982-2001) derived from CMAP rainfall (Xie and Arkin 1997) and Reynolds (Reynolds et al. 2002) SST. The simulated results were made by 5 AGCM's multi-model ensemble hindcast.

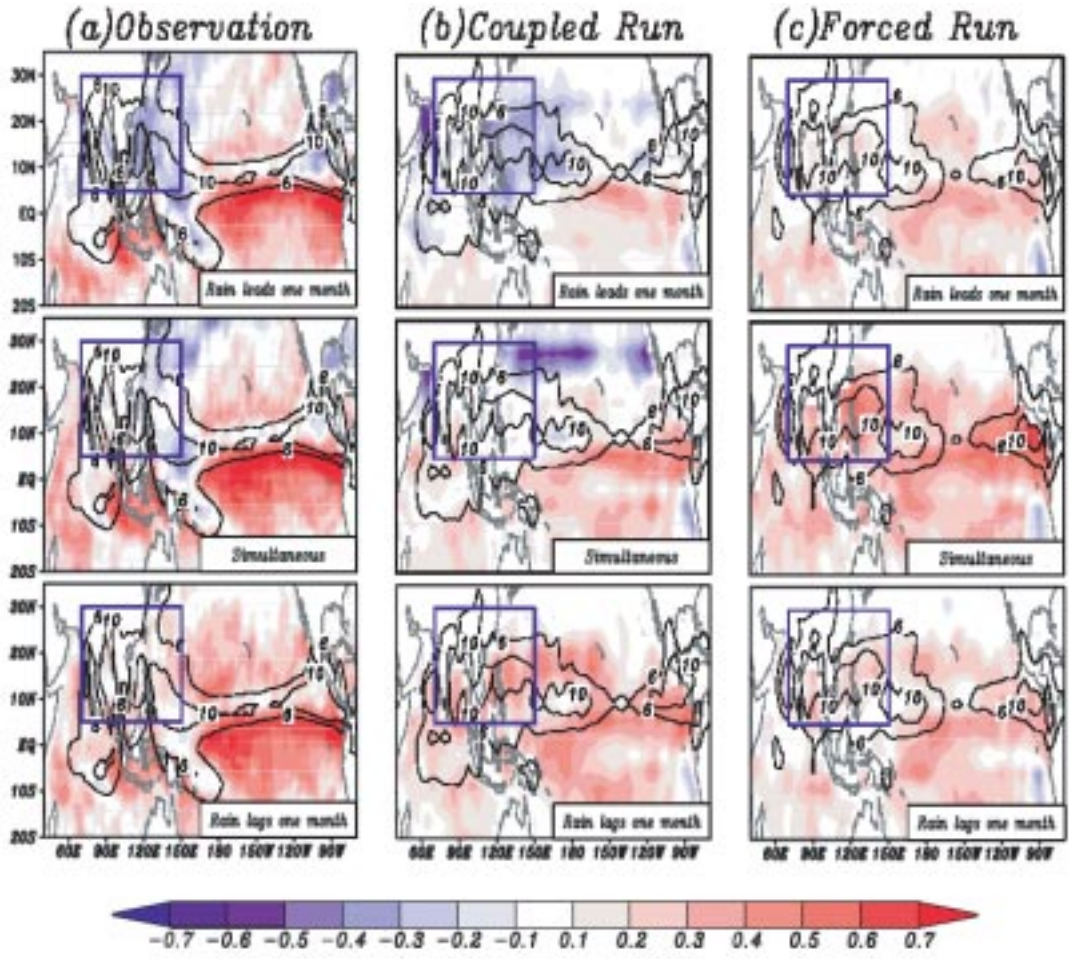

Fig. 3 (a) Observed lead-lag correlation coefficients between monthly mean SST and precipitation anomalies computed for May through October of 1982-2001. The top, middle, and bottom panel represents the correlation coefficients when precipitation leads SST by one month, is concurrent with SST, and lags SST by one month, respectively. The sample size is 80 for the time series at each grid. (b) The same as in (a) except that the correlations were computed from the coupled ECHAM-ocean model simulation. (c) The same as in (a) except that the correlations were computed from the forced ECHAM simulation

From Zhao et al, Page 11: Seasonal and annual predictions of sea surface temperature anomalies over the tropical Pacific Ocean by using a multi-models system

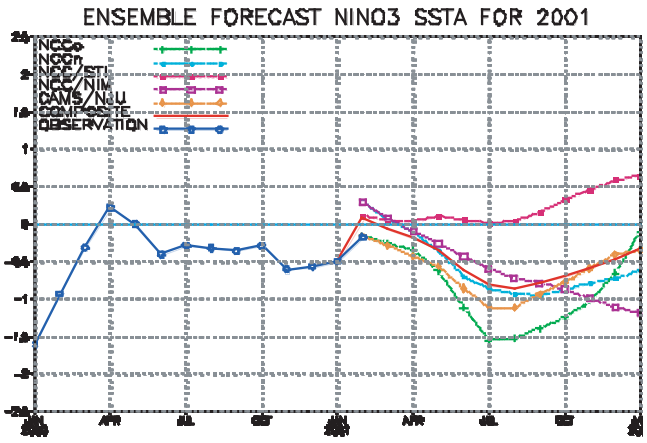

Fig.1 Multi-seasonal predictions of Nino3 index for March 2001 ~ January 2002 (Li, 2001)

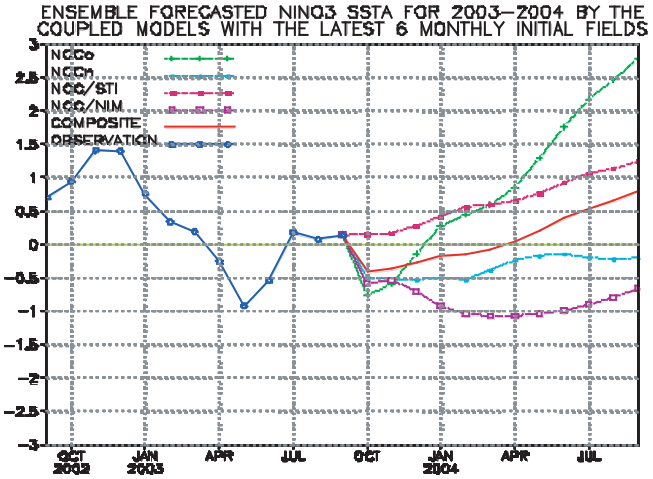

Fig.2 Multi-seasonal predictions of Nino3 index for October 2003 ~ September 2004 (Zhang, 2003)

From Chaves and Ambrizzi, page 24: Atmospheric response for two convection schemes in sensitivity experiments using SST anomalies over the South Atlantic Ocean

Figure 1 - Rainfall rate (mm/day; shaded) and SST (ºC; contour) for (a) CTRK, *(b)* CK, *(c)* WK, *(d)* CRTA, *(e)* CA *and (f)* WA *experiments.*

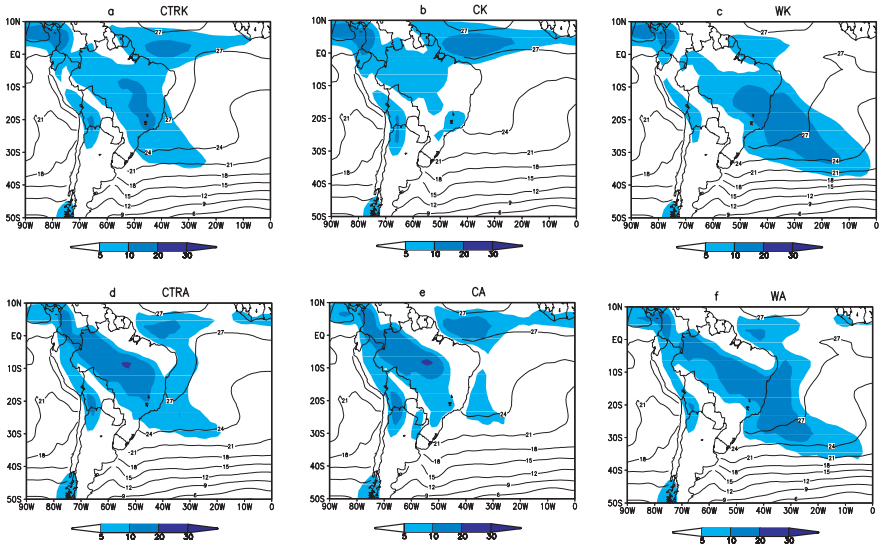

From Gerdes et al page 27: Reaction of the oceanic circulation to increased melt water flux from Greenland - a test case for ocean general circulation models

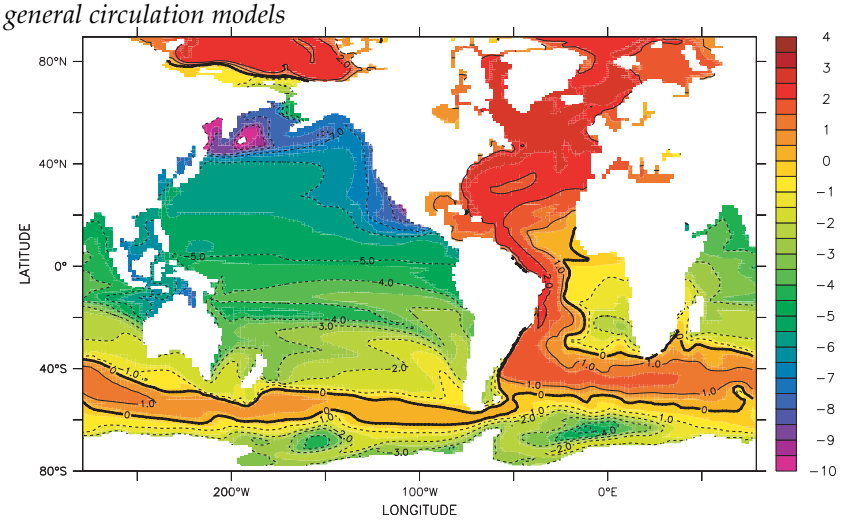

Fig. 2. Logarithm of the (negative) vertical integral of the passive salinity anomaly tracer in the EBM experiment. The tracer shows the direct effect of the fresh water flux anomaly around the coasts of Greenland. The figure shows the average over the last twenty years (80-100) of the experiment.

From Silva et al, Page 23: CLIVAR Science: application to energy: The 2001 energy crisis in Brazil

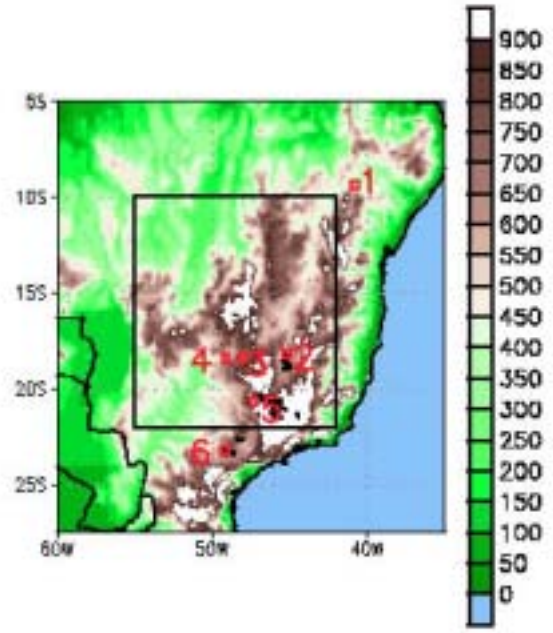

Figure 1. Elevation (mm) for tropical South America. The box (10°-22°S, 42°-55°W) includes the headwater regions for major rivers flowing into the 1) Tocantins, 2) São Francisco, and 3) Paraná/ La Plata basins. The numbers on the map indicate the locations of the following water reservoirs: 1) Sobradinho, 2) Três Marias, 3) Emborcação, 4) Itumbiara, 5) Furnas, and 6) Jurumim.

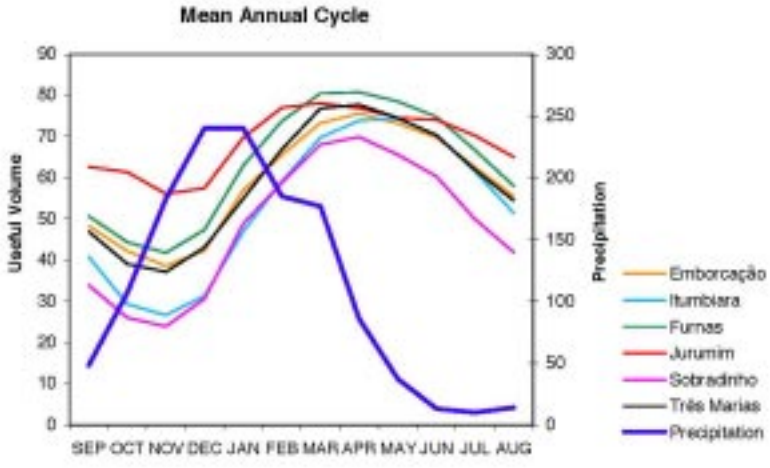

Figure 2. The mean annual cycle of precipitation (mm) for central Brazil (10°-22°S, 42°-55°W), as indicated in Fig. 1, and the mean annual cycle for the useful water volume (%) for the six reservoirs. The useful volume is the water volume between the maximum and minimum levels for which the dam can produce electricity

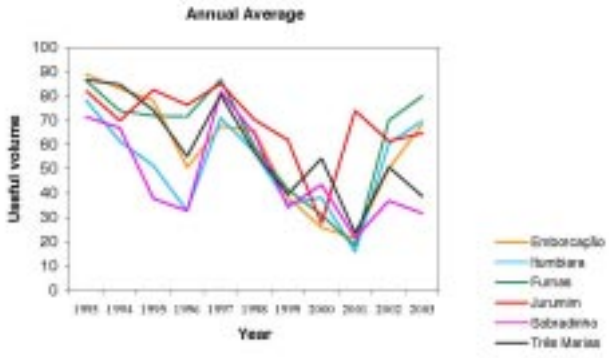

Figure 3. Useful volume annual average (%) from 1993 to 2003 for reservoirs indicated in Fig. 1. The useful volume is the water volume between the maximum and minimum levels for which the dam can produce electricity.

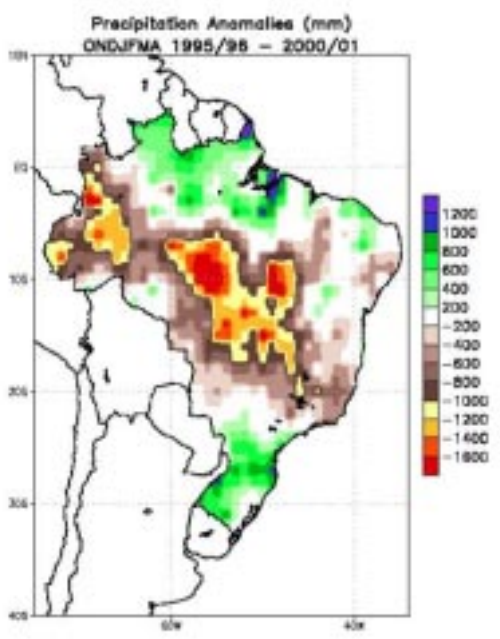

Figure 4. Mean anomalous precipitation for October-April 1995/96 to 2000/01. Data are derived from the daily gridded analyses of precipitation produced by the NOAA/ Climate Prediction Center

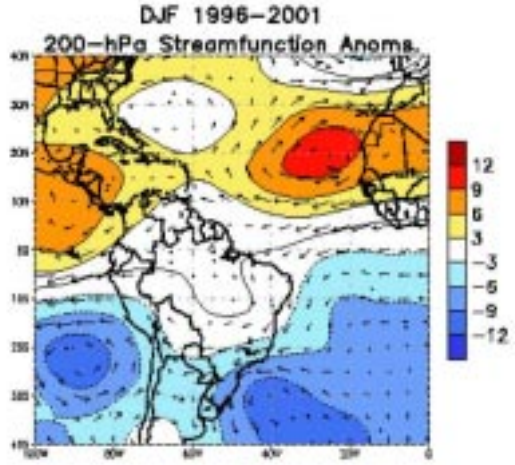

Figure 6. Six-year average 200-hPa streamfunction (shading) and vector wind anomalies for December-February (DJF). Negative streamfunction anomalies (blue shading) in the SH and positive streamfunction anomalies (orange and red shading) in the NH indicate anomalous anticyclonic circulation. The base period used for computing the anomalies is 1979-1995. Units for stream function are 10^6 m s

Continued from page 14

Raw and adjusted skill of ECHAM 4.5 and ARPEGE

Figure 1 displays the one–point correlation between SRI_{obs} and the observed gridded rainfall (Figure 1a), then with ARPEGE (Figure 1b) and ECHAM 4.5 (Figure 1c) simulated rainfall. Concerning observations (Figure 1a), the zonal consistency of the Sahelian rainfall variability is striking with correlations over 0.5-0.6 stretched eastward outside the SRI box, to the Red Sea. Note also large positive correlations over Guinean mountains and also over the Southern Chad and the Sudan (Figure 1a). The correlations between SRI_{obs} and ARPEGE rainfall (Figure 1b) match the observed pattern quite well, with a slight northward shift. The correlations are also weaker over the western part of the SRI box (Figure 1b). The maximum in the correlations between SRI_{obs} and ECHAM 4.5 simulation (Figure 1c) are slightly southward shifted over central Sahel, with a large northeastward extension of positive correlations over the eastern Sahara (Figure 1c). Even if the correlations inside the SRI box are significant, slight shifts of the pattern occur for both AGCMs. When the same boundary limits as in observation are considered, the correlations between SRI_{obs} and simulated SRI are significant at the 0.01 one-sided level, but the skill is largely due to decadal variability and trends (Table 1). At high-frequency time scales (Table 1), the correlations are not significantly different from zero for both AGCMs. Both AGCMs remain significantly correlated with each other on LF but also on HF time scale (Table 1), suggesting that the SST-forced component is quite robust and almost unconditional upon the AGCM used.

The spatial shift of the teleconnection observed in Figure 1b and 1c, could be easily corrected by a linear method such as Canonical Correlation Analysis (CCA). Model outputs are adjusted based on the leading two CCA modes between the large-scale (i.e. concatenated runs on 50°W-50°E and 0°-35°N) simulated rainfall and the regional-scale observed rainfall inside the SRI box (Ward and Navarra, 1997 ; Moron *et al.*, 2001). To avoid overfitting, 5 years from 1950 to 1996 are held out in turn and CCA is used to develop a prediction model using the remaining 42 years. The temporal correlation between the CCA cross-validated hindcasts and SRI_{obs} is improved, mainly at HF time scale (Table 1). In the following, SRI_{arp} and SRI_{echam} refer to simulated rainfall obtained from the CCA cross-validated hindcasts.

The skill for each year is evaluated using the Rank Probability Skill Score –RPSS hereafter-(Doblas-Reyes *et al.*, 2000). Rank Probability Score (RPS, Epstein, 1969) is here defined with terciles (SRI_{obs} time series is divided into three categories having respectively 16,15 and 16 members and SRI_{arp} and SRI_{echam} are ranked into these categories). RPS is referred to climatology to give RPSS, which represents a percentage improvement in RPS over the 1950-1996 climatology. A RPSS of 100% means that all runs are in the same class as the observed value. A negative RPSS indicates skill worse than climatology. RPSS is below zero in 1960, 1973, 1976, 1981, 1985, 1988, 1993, 1994 and 1995 for both AGCMs, 1970, 1979, 1987, 1990 for ARPEGE only and 1951, 1965, 1966, 1969, 1977, 1978, 1996 for ECHAM only (Figure 2). It seems that the unskillful years are thus concentrated during the dry period, from 1968. On the contrary, the most

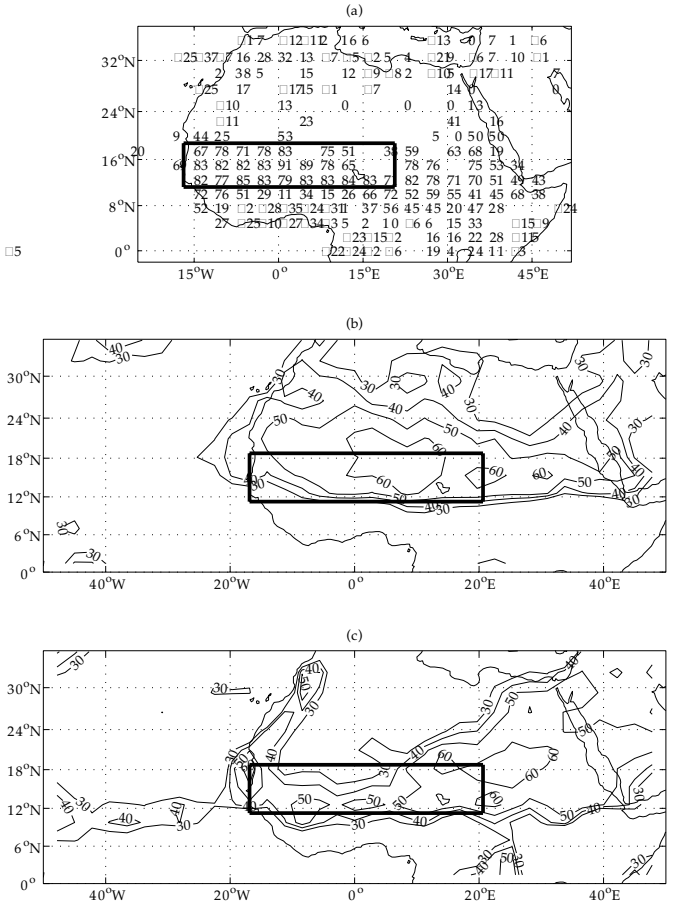

Figure 1 : correlation (x 100) maps between SRI_{obs} and (a) observed JAS seasonal rainfall (from CRU dataset) ; (b) simulated JAS seasonal rainfall (mean ensemble from ARPEGE) ; (c) simulated JAS seasonal rainfall (mean ensemble from ECHAM 4.5). In panels (b) and (c), contours are traced at 30, 40, 50 and 60 only. The SRI box is contoured on each map

skillful years, having a RPSS over 50%, occur mostly during the wet period, till 1967 (Figure 2).

The origin of errors could be various. First of all, it is known that the observed network deteriorates from the 1970s. Fewer stations could decrease the signal-to-noise ratio of the regional index and thus make it less predictable. The CPC merged analysis of precipitation (CMAP) dataset, from gauge data and satellite estimates, could be used as an alternative of the surface CRU dataset. The data are available from 1979 on a 2.5 x 2.5 grid. The SRI computed from the CMAP dataset is correlated at 0.93*** (in the following, one, two and three stars indicate significant correlations at the one-sided 0.1, 0.05, 0.01 levels according to a random-phase test (Janicot *et al.*, 1996) with 10000 random time series) with SRI_{obs} on the 1979-1996 period and no systematic increase of the difference between both indices is observed (not shown), suggesting that the decrease of the skill of the AGCMs may not be related to the deterioration in the observed network. Of course, these errors could be due to sampling variations but the apparent concentration of the unskillful years during the dry period for both AGCMs is intriguing. Firstly, the AGCM could be wrong in the transmission of a particular SST forcing onto the atmosphere,

	Obs vs ECHAM	Obs vs ARPEGE	ECHAM vs ARPEGE
Correlation	0.59***	0.58***	0.78***
SST-forced variance (%) of AGCM runs	24.5	49	.
LF Correlation	0.89***	0.74**	0.89***
LF SST-forced variance (%) of AGCM runs	48.4	73.1	.
HF Correlation	0.03	0.24	0.68***
HF SST-forced variance (%) of AGCM runs	13.5	31.4	.
Correlation after CCA correction of AGCM runs	0.70***	0.70***	0.82***
SST-forced variance (%) after CCA correction of AGCM runs	62	56.2	.
LF Correlation after CCA correction of AGCM runs	0.88***	0.80***	0.92***
LF SST-forced variance (%) after CCA correction of AGCM runs	78.7	82.5	.
HF Correlation after CCA correction of AGCM runs	0.40**	0.43***	0.66***
HF SST-forced variance (%) after CCA correction of AGCM runs	49.5	29.1	.

Table 1 : Cross-correlations and externally SST-forced variance (Rowell et al.*, 1995) between observed and simulated SRI. The scores are given for the direct AGCM outputs at low-frequency (LF) and high frequency (HF) time scales and for the CCA-adjusted AGCM outputs . One, two and three stars indicate significant correlations at the one-sided 0.1, 0.05 and 0.01 level using a random-phase test (Janicot* et al.*, 1996) with 10000 random time series. The null hypothesis is that correlation is zero and the alternative hypothesis is that correlation is positive.*

because of its own over- or under-sensitivity. It is possible that these years exhibit a particular combination of SST anomalies and/or are dominated by a SST anomalies pattern that is not properly transmitted to the atmosphere. There could be also some cancellation effect between different SST forcings. Figure 3 (page 22) displays the observed standardized SST anomalies in July-September for four sets of years according to the sign of ensemble mean of SRI_{arp} or SRI_{echam} and the RPSS > 50% (< 0%) defines a skillful (unskillful) year. Note that considering a threshold of 0% rather than 50% to define the skillful years doesn't change the SSTA pattern displayed on Figure 3. The SSTA pattern during the skillful years (Figure 3a,b,e,f) and the unskillful years (Figure 3c,d,g,h) are usually different. The SSTA pattern during the unskillful years is usually noisier, with few areas achieving a local significance (Figure 3c,d,g,h). In particular, mean SSTAs over the Tropical Pacific are quite weak (Figure 3c,d,g,h), whereas they are quite strong during the skillful years (Figure 3a,b,e,f). It is then difficult to conclude about the sensitivity of both AGCMs to particular SST patterns and an individual case analysis is needed because SSTAs are highly variable during the unskillful years (not shown). The occurrence of unskillful year could be also related to a dominant forcing other than SST. In that context, it is interesting to compare the results of the AGCMs with a statistical hindcast of SRI using the global SST. A cross-validated CCA (with 5 years held out at each turn) is used with the predictand being the observed gridded rainfall inside the SRI box and the predictor being the near-global seasonal observed SST (60°S-70°N) in July-September. The principal predictor map for CCA mode 1 (Figure 4a) reveals the well-known teleconnection SST pattern associated with SRI variability. Note that loadings for both CCA modes are quite weak over the Tropical Northern Atlantic and central and eastern parts of the Tropical Southern Atlantic (Figure 4a,b). The leading two CCA modes are used to hindcast gridded observed rainfall inside the SRI box from the global SST. The mean of the standardized hindcast inside the SRI box (Figure 4c) is referred as SRI_{sst} hereafter. The correlation between SRI_{obs} and SRI_{sst} is 0.79*** ($r(SRI_{obs}, SRI_{sst})$ = 0.89*** at LF time scale and $r(SRI_{obs}, SRI_{sst})$ = 0.55*** at HF time scale). More interestingly, if SRI_{sst} is ranked into the three classes defined above from SRI_{obs}, 7 out of 9 years that are not properly simulated by any AGCMs (RPSS < 0% for both AGCMs) are also wrongly classified with the statistical hindcast scheme. In the same order of idea, the correlation between simulated SRI and SRI_{sst} for years having a negative RPSS are significant ($r(SRI_{arp}, SRI_{sst})$ = 0.55*** (13 years) and $r(SRI_{echam}, SRI_{sst})$= 0.72*** (16 years)). In other words, neither a dynamical nor a statistical linear model is able to reproduce accurately the observed SRI during these years.

Conclusion and future directions

The correlation between SRI_{obs} (defined as the mean of the standardized anomalies inside a regional area : 16°W-20°E ; 11.25°-18.75°N) and simulated SRI is around 0.58*** for ARPEGE and ECHAM 4.5 and reaches a level of 0.70*** for both AGCMs after a statistical correction. As demonstrated elsewhere, it seems that SST provides the major forcing of the long-term decreasing trend during the second half of the twentieth century (e.g. Rowell *et al.*, 1995 ; Giannini *et al.*, 2003). Nevertheless, at HF (< 8 years) time scales, the correlation is statistically significant after the CCA correction (*r.* between SRI_{obs} and simulated SRI > 0.4**), and both AGCMs are strongly consistent between them (*r*. between SRI_{arp} and SRI_{echam} > 0.66***). In other words, it seems that the SST-forced component (as extracted from the mean ensemble) is quite robust, even at the HF time scale.

The unskillful years, identified here through a negative RPSS, are concentrated during the dry long-term period (from 1968), even when the leading wet years, in particular during the 1950s and the beginning of the 1960s, are correctly simulated. This temporal modulation could partly explain the low skill scores recorded during the first "Atmospheric Model Intercomparison Project" experiment (1979-1988) (Sperber and Palmer, 1996). A CCA statistical model using near-global SST as predictor is not able either to properly hindcast observed SRI during these unskillful years. We could hypothesize that

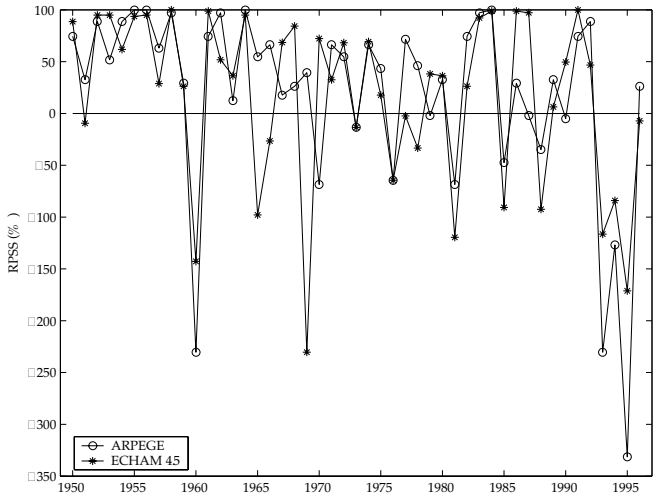

Figure 2 : RPSS (in %) for SRI_{arp} (full line with circle) and SRI_{echam} (full line with asterisk). The RPS is defined from three classes having respectively 16, 15 and 16 members.

the occurrence of these unskillful years is not just associated with the sampling variability related to the fact that 100% of the temporal variance of SRI isn't SST-forced. Observed Sahelian rainfall anomalies during the unskillful years, may be strongly forced by ; (i) a particular SST pattern that isn't accurately transmitted to the atmosphere by the AGCM for any reason - these SST patterns should include localized SSTA or specific uncommon combination of SSTA ; and/or (ii) continental surfaces.

Acknowledgments

The ARPEGE outputs were kindly provided by L. Terray (Cerfacs, Toulouse). Thanks also to Andy Robertson (IRI) for his careful review and friendly support.

Reference

Cassou C., and L. Terray, 2001 : Influence of tropical and extratropical SST on inter-annual atmospheric variability over the North Atlantic, *J. Climate*, **14**, 4265-4280.

Doblas-Reyes F., M. Deque, and J.P. Piedelievre, 2000 : Multi-model spread and probabilistic seasonal forecast in PROVOST. *Quart. J.R.Meteo. Soc.*, **126**, 2069-2087.

Epstein E.S., 1969 : A scoring system for probabilistic forecasts of ranked categories. *J. Appl. Meteorol.*, **8**, 985-987.

Giannini A., R. Saranavan, and P. Chang, 2003 : Oceanic forcing of Sahel rainfall on inter-annual to interdecadal time scales, *Science*, **302**, 1027-1030.

Gong X., A.G. Barnston, and M.N. Ward, 2003 : The effect of spatial aggregation on the skill of seasonal precipitation forecasts. *J. Climate*, **16**, 3059-3071.

Janicot S., V. Moron and B. Fontaine, 1996 : Sahel droughts and ENSO dynamics. *Geophys. Res. Letters*, **23**, 515-518.

Katz, R.W., Glantz M.H., 1986, Anatomy of a rainfall index. *Monthly Weather Review* **114,** 764-771.

Moron V., A. Navarra, and N.M. Ward, 2001 : Observed and SST-forced seasonal rainfall variability across Tropical America. *Int. J. Climatol.*, **21**, 1567-1601.

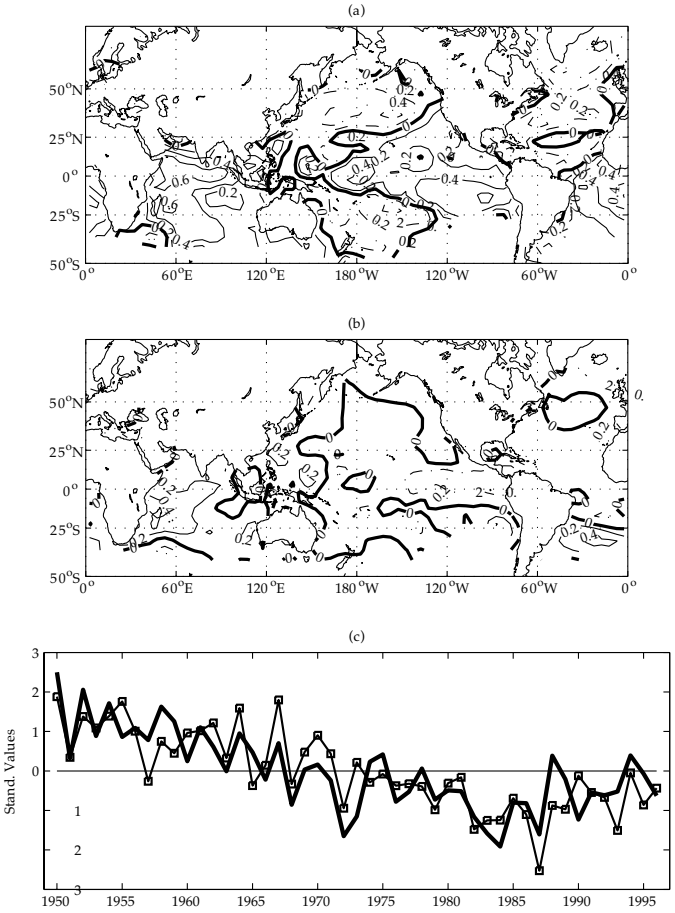

*Figure 4 : Geographical distribution of the correlation between observed SST and rainfall time series of mode 1 (a) and mode 2 (b) of a cross-validated (5 years are held out in turn) CCA using observed July-September gridded rainfall inside SRI box as predictand and observed July-September global SST (on a 5 x 5 grid) as predictor. Contour interval is 0.20 and negative contours are dashed-dotted. The correlation between time series associated with mode 1 (2) equals 0.82*** (0.27*). (c) standardized time series of SRI_{obs} (bold line) and SRI_{sst} (line with square). SRI_{sst} is the mean of the standardized anomalies obtained from the CCA between the global SST and the gridded rainfall inside SRI box.*

Moron V., N. Philippon, and B. Fontaine, 2003 : Skill of Sahel rainfall variability in four atmospheric GCMs forced by prescribed SST, *Geophys. Res. Letters*, **30**, DOI:10.129/2003GL018006.

Moron V., N. Philippon, and B. Fontaine, 2004 : Simulation of West-African monsoon circulation in four atmospheric general circulation models forced by prescribed sea surface temperature. *J. Geophys. Res.*, **109**, D24105, DOI:10.1029/2004JD004760.

Rowell D.P., C.K. Folland, K. Maskell, and M.N. Ward, 1995 : Variability of summer rainfall over Tropical North Africa (1906-1992) : observations and modeling. *Quart. J.R.Meteo. Soc.*, **113**, 669-674.

Sperber K.R., and T.N. Palmer, 1996 : Inter-annual tropical rainfall variability in general circulation model simulations associated with the Atmospheric Model Intercomparison Project, *J. Climate*, **9**, 2727-2750.

Tippett M.K., R. Kleeman, and Y. Tang, 2004 : Measuring the potential utility of seasonal climate prediction. *Geophys. Res. Letters*, **31**, DOI : 10.109/2004GLO21575.

Thiaw W.M., A.G. Barnston, and V. Kumar, 1999 : Predictions of african rainfall on the seasonal time scale. *J. Geophys. Res.*, **104**, D24, 31589-31597.

Ward.M.N., 1998 : Provisionally corrected surface wind data, worldwide ocean-atmosphere surface field and sahelian rainfall variability. *J. Climate*, **11**, 3167-3191.

Ward M.N., and A. Navarra, 1997 : Pattern analysis of ensemble GCM simulations with prescribed SST : boreal summer examples over Europe and the tropical Pacific. *J. Climate*, **10**, 2210-2220.

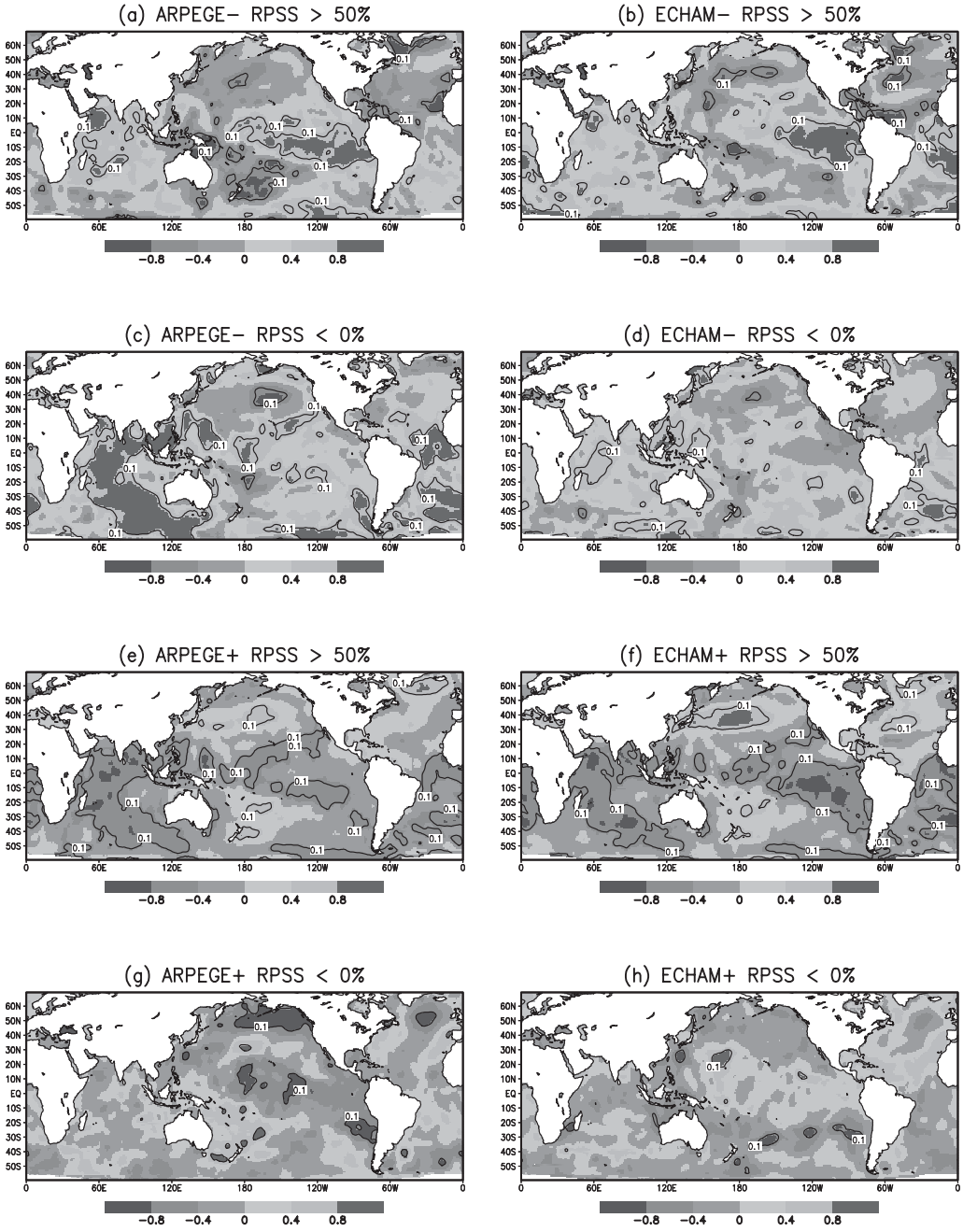

Figure 3 : Observed July-September standardized SST anomalies (relative to the mean and standard deviation of the 1950-1996 period) for (a) skillful dry years for ARPEGE (RPSS of $SRI_{arp} > 50\%$ and mean ensemble anomaly of $SRI_{arp} < 0$) ; (b) skillful dry years for ECHAM (RPSS of $SRI_{echam} > 50\%$ and mean ensemble anomaly of $SRI_{echam} < 0$) ; (c) unskillful dry years for ARPEGE (RPSS of $SRI_{arp} < 0\%$ and mean ensemble anomaly of $SRI_{arp} < 0$) ; (d) unskillful dry years for ECHAM (RPSS of $SRI_{echam} < 0\%$ and mean ensemble anomaly of $SRI_{echam} < 0$) ; (e) skillful wet years for ARPEGE (RPSS of $SRI_{arp} > 50\%$ and mean ensemble anomaly of $SRI_{arp} > 0$) ; (f) skillful wet years for ECHAM (RPSS of $SRI_{echam} > 50\%$ and mean ensemble anomaly of $SRI_{echam} > 0$) ; (g) unskillful wet years for ARPEGE (RPSS of $SRI_{arp} < 0\%$ and mean ensemble anomaly of $SRI_{arp} > 0$) ; (h) unskillful wet years for ECHAM (RPSS of $SRI_{echam} < 0\%$ and mean ensemble anomaly of $SRI_{echam} > 0$). The two-sided 0.1 level significance according to a Student's t test is contoured (null hypothesis : SST are equal to the long-term (1950-1996) climatology) on each map.

CLIVAR Science: Application to energy: The 2001 Energy Crisis in Brazil

Viviane B. S. Silva[1], Vernon E. Kousky[2], Antonio J. Busalacchi[3]
[1]Department of Meteorology, University of Maryland
[2]Climate Prediction Center (NOAA/CPC), Camp Springs
[3]Earth System Science Interdisciplinary Center (ESSIC), University of Maryland
Corresponding author: vsilva@atmos.umd.edu

1. Introduction

In 2001 Brazil experienced a major energy crisis that led to the implementation of restrictions on energy usage throughout the country in order to avoid large-scale blackouts. Three main factors contributed to the energy crisis: 1) prolonged drier-than-average conditions, which lasted up to six years (1996-2001) in the upper portion of the Tocantins, São Francisco and La Plata/Paraná river basins (see box in Figure 1, page 18), 2) increasing energy demands, and 3) delays in implementing new power plants (Kelman et al., 2001).

In 2002 about 85% of the Brazilian total energy production was generated by hydroelectric power plants. The electricity-generating system of Brazil consists of a) an integrated network, connecting the South, Southeast, and Central regions (SSEC), b) an integrated network, connecting the North and Northeast regions (NNE), and c) about 300 individual generating facilities mainly in North Brazil. The integrated network SSEC allows for a seasonal exchange of energy within the region, with energy flowing toward the Southeast and Central-West during the dry season (May-November) in those regions and toward the South during the remainder of the year. The integrated network NNE also displays seasonality in the energy exchange within the region, with flows toward the Northeast during the first half of the year, when there is an abundance of water in the Tocantins River basin. The flow is reversed during the second half of the year when the Tocantins River is at its lowest levels (Silveira, et al. 1999).

The mean annual cycles of precipitation for Central Brazil and the useful volume (water volume between the maximum and minimum levels for which the dam can produce electricity) for major reservoirs in the region (Figure 2, page 18) show that there is a 3-5 month lag between the time of the year when precipitation is maximum and the time when the useful volume reaches a maximum.

The hydroelectric system of Brazil is designed to satisfy the energy demands in the case of successive dry years (Kelman et al. 2001). However, at the end of April 2001, the useful volume of water stored in most of the reservoirs in the Southeast, Central-West and Northeast regions was between 20% and 30% of the maximum (Figure 3, page 18), which was insufficient to satisfy projected energy demands for the remainder of the year. The decrease in the useful volume was partly due to the continued production of energy to meet increasing demands and partly due to prolonged drier-than-average conditions over most of Brazil. The combined effect of increased energy demand and reduced water availability contributed to the 2001 energy crisis.

To avoid large-scale blackouts the Brazilian government implemented a program during the last half of 2001 to drastically reduce energy consumption. The program's goal was to reduce energy consumption by 1) 20% for residential consumers who consumed more than 100KWh/month, 2) 20% for commercial consumers, and 3) 20% to 25% for industrial consumers. Each consumer was allowed to decide when and how to save energy. The reduction plan was based on energy used during May, June and July of the previous year. In order to encourage consumer involvement in the program, the government established a fine for those who did not meet the reduction guidelines and gave credits to those who met the guidelines. The whole country participated in the plan leading to a successful program (Pires et al., 2002).

The amount of hydroelectric power generation in Brazil steadily increased from 1990 to 2000 (Table 1). During 2001 there was approximately a 12% decrease in power generation compared to the previous year. In 2002, there was once again an increase in the power generation, but the amount generated remained below the level produced in 2000.

In this paper we will focus on the climate variability aspect of the Brazilian energy crisis, although for planning and management purposes all three factors: 1) prolonged drier-than-average conditions, 2) increasing energy demands, and 3) delays in implementing new power plants, must be considered.

2. Climate variability aspect of the energy crisis

The South American monsoon system (SAMS) has been a major focus of the CLIVAR/ VAMOS (Variability of the American Monsoon System) program. The core of SAMS is located over the high plains (planalto) region of Central Brazil (see box in Figure1), which is also the source region for major rivers flowing into three different basins (north into the

	1990	1991	1992	1993	1994	1995	1996	1997	1998	1999	2000	2001	2002
Net Generation	204.6	215.6	221.1	232.7	240.3	251.4	263.1	276.2	288.6	290.1	301.6	265.2	282.1

Source: Carbon Sequestration Leadership Forum

Table 1. Hydroelectric Power Generation in Brazil, 1990-2002 (in billions of kilowatt-hours).

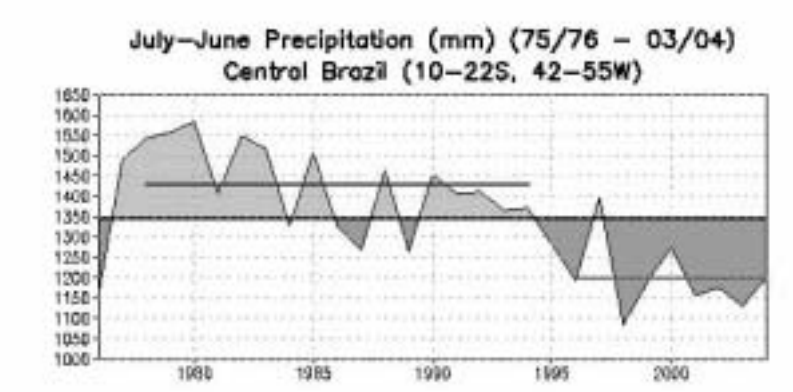

Figure 5. Time series of total (July-June) precipitation (mm) for the box in Fig. 1. The base period for computing the long-term average (1350 mm) is July1975-June 2003. The blue line indicates the average precipitation for July 1977-June 1978 through July 1993-June 1994 and the red line indicates the average precipitation for July 1995-June1996 through July 2003-June 2004. The totals were computed for the period July-June in order to represent the entire hydrological water year.

Amazon, northeast into the São Francisco, and south into the La Plata).

The mean precipitation anomalies for October - April from 1995-96 through 2000-01 (Figure 4, page 18) show large deficits of precipitation over central and southeastern Brazil, which are important regions for water storage and hydroelectric energy generation. The precipitation time series (July-June) (Figure 5) for Central Brazil (see box in Figure 1), shows that during 1977 through 1994 precipitation was above the 1975-2003 mean value (1350 mm) for the entire period, except for 1986, 1987, and 1989. For the period 1995 to 2004, the mean average precipitation was about 1200 mm, which shows a reduction of about 16% compared with the previous period (1977-1994). It is noteworthy that the mean precipitation during the recent dry period is less than the minimum amount of precipitation that occurred any year during 1977-1994. The prolonged nature of the dryness (1996-2001) played a major role in the 2001 energy crisis in Brazil.

The mean December-February (DJF) upper-tropospheric anomalous circulation (streamfunction and vector wind) pattern for the period 1996-2001 (Figure 6, page 18) shows anticyclonic circulation over low-latitudes of the eastern South Pacific and South Atlantic, indicating weaker-than-average climatological troughs in those regions. At low-latitudes over tropical South America the anomalous flow is cyclonic, indicating a weaker-than-average Bolivian anticyclone. All of these circulation features (weakened troughs over the Pacific and Atlantic, weakened Bolivian high) indicate a weaker-than-average SAMS during the six-year period DJF 1995/96-2000/01, which is consistent with the drier-than-average conditions observed over Central Brazil during the period (Figures 4 and 5).

The circulation anomalies in the Northern Hemisphere are mirror images of those in the Southern Hemisphere. In both hemispheres there is anomalous anticyclonic flow in the subtropics. This large-scale anomalous circulation pattern has been associated with other decadal circulation changes in the region of the North Atlantic, such as increased tropical SST anomalies and increased hurricane activity since the mid-1990s (Figure 7) (Goldenberg et al. 2001; Bell et al. 2004). It is noteworthy that the average SST anomaly for the period 1979-

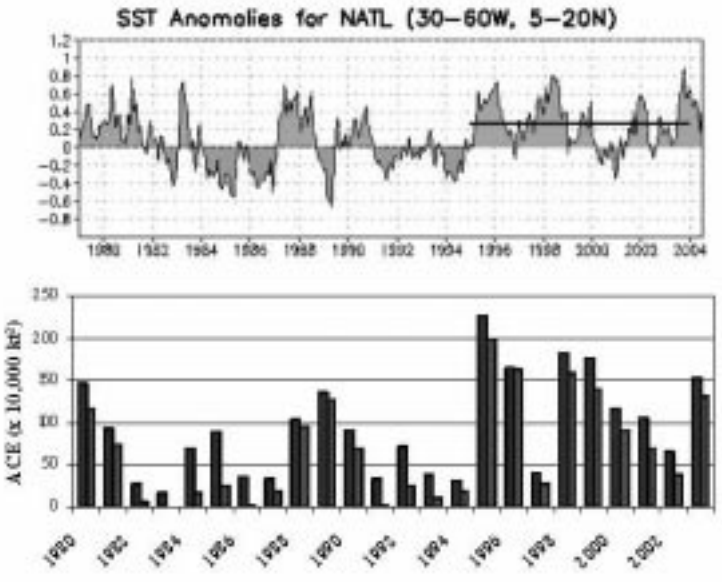

Figure 7. Sea surface temperature (SST) anomalies (top panel) for the tropical North Atlantic (anomalies were computed with respect to the 1971-2000 base period), and tropical Accumulated Cyclone Energy (ACE) (bottom panel) for the entire Atlantic basin (left hand column) and for the main development region (MDR) (righthand column). Figure adapted from Bell et al. (2004). MDR is defined as tropical Atlantic and Caribbean Sea between 9°- 21.5°N.

1994 is zero, while the average for the period 1995-2003 is approximately +0.3ºC.

3. Conclusion

One of the CLIVAR goals is to understand the physical processes responsible for climate variability and predictability. Through increased understanding of those processes the CLIVAR community will be able to provide information about climate variability that will lead to improved planning. Countries that rely heavily on hydroelectric power need to have information on the full range of interannual-to-decadal precipitation variability that can be expected, in order to develop adequate plans for future water usage and energy generation. In order to respond to energy demand, a lead-time prediction capability for the rainfall variability in the region will be one among several factors to be taken into account in planning future water resource allocations and development of new infrastructure. In the case of Brazil, rainfall variability was an important factor for the 2001 crisis, but inadequate planning was also a contributing factor. Brazil is still in a vulnerable position and could face future energy crises because we do not yet have a firm understanding of the causes for interannual-to-decadal climate variability in precipitation and its potential predictability for the region of SAMS. Even with a 100% accurate prediction of future rainfall variability there will still be societal limitations on the utility of such forecasts. The recent experience shows the need for improved links between predictions of the physical climate systems and the human dimension aspects of the socio-politic-economic sectors. Even if the rainfall forecast for Brazil were perfect, given the nature of the hydroelectric industry in Brazil as we described, the implementation and application of those forecasts would have limits. Improved planning is needed in order to take into account the full range of natural climate variability, as well as to anticipate changes in climate that might occur in the future due to global warming.

In this paper we gave a brief overview of the 2001 energy crisis in Brazil and presented some evidence indicating that large-scale decadal climate variability contributed to the lack of water resources leading up to the crisis. Additional work is necessary to determine how the large-scale circulation changes, documented here, are linked to the frequency and intensity of the weather disturbances that affect rainfall.

Acknowledgments

The authors would like to thank the ONS (Operador Nacional do Sistema Elétrico) in Brazil for providing the useful volume data. The first author greatly appreciates the comments and suggestions of Rafael C. Di Bello from the Agência Nacional de Águas (ANA).

References:

Bell, G. D., S. Goldenberg, C. Landsea, E. Blake, R. Pasch, M. Chelliah, and K. Mo, 2004: State of the Climate in 2003. Section: Tropical storms – Atlantic hurricane season. *Bull. Amer. Meteor. Soc*., **85,** S20.

CLSF - Carbon Sequestration Leadership Forum: An Energy Summary of Brazil. Last updated January 15, 2004 (www.cslforum.org/press_brazil.htm)

Goldenberg, S. B., C. W. Landsea, A. M. Mestas-Nuñez, and W. M. Gray, 2001: The recent increase in Atlantic hurricane Activity. *Science*, **293**, 474-479.

Kelman, J., A. Venture, S. V. Bajay, J. C. Penna, and C. L. S. Haddad, 2001: Relatório da Comissão de Análise do Sistema Hidrotérmico de Energia Elétrica: O desequilíbrio entre oferta e demanda de energia elétrica.: *Agência Nacional de Águas/ANA*. Brasília 21 July 2001.

Pires, J. C., F. Giambiagi, A. F. Sales, 2002: As perspectivas do setor elétrico após o racionamento. *Revista do BNDES, Rio de Janeiro*, **9,** 163-204.

Silveira, C. A. C., L. Mejia, R. S. A. Ferreira, L. G. F. Guilhon, O. B. Silva, and M. A. V. Freitas, 1999: Água e energia elétrica. *Aneel publication - O Estado das Águas no Brasil*., 103-115

Atmospheric response for two convection schemes in sensitivity experiments using SST anomalies over the South Atlantic Ocean

Rosane Rodrigues Chaves and Tércio Ambrizzi
Universidade de São Paulo, Insituto de Astronomia, Geofisica e Ciencias Atmmosfericas
Corresponding author: rosane@io.met.fsu.edu

Abstract

This study indicates how different convective schemes can influence the response of sensitivity experiments with prescribed Sea Surface Temperature (SST) over the South Atlantic Ocean using the CPTEC/COLA AGCM. The Kuo and Relaxed Arakawa and Schubert (RAS) schemes are used. The experiments with both schemes show that warm SST anomalies over the South Atlantic Ocean tend to intensify the South Atlantic Convergence Zone (SACZ), while cold SST anomalies have an inverse effect. However, rainfall patterns over most of South America are less intense with Kuo than with RAS scheme in all experiments. Positive SST anomalies tend to move northward the SACZ in the Kuo experiment and for the RAS scheme its location is independent of the SST anomalies over the South Atlantic Ocean. An inverse relationship between the SACZ and ITCZ in terms of precipitation intensity is observed to positive SST anomalies with Kuo scheme. This association is not observed with the RAS scheme.

1. Introduction

The focus of this work is to show how different convective parameterizations can influence the results of sensitivity experiments with prescribed SST over the South Atlantic Ocean with the CPTEC/COLA AGCM. A complementary study of the numerical results of Chaves

and Nobre (2004) is presented here where the dependence of their results on the convective scheme used in the atmospheric model is investigated. As the South American atmospheric circulation is very sensitive to the location and intensity of the heating rates (Silva Dias et al. 1983), the use of different cumulus parameterization schemes can cause different atmospheric responses for convection schemes in sensitivity experiments using SST anomalies over the South Atlantic Ocean. Thus, the impact of different convection schemes in the context mentioned above is very important.

2. Material and methods

Six experiments for the period November 2000 to February 2001 were carried out in order to investigate how different convective schemes can influence the results of sensitivity experiments with prescribed SST over the South Atlantic Ocean. The South Atlantic SST fields appropriate to cold and warm experiments are computed using the expressions (1) and (2), respectively:

$$SST_C = SST_{CTR} - [1+abs(SSTA_{CTR})] \quad (1)$$

$$SST_W = SST_{CTR} + [1+abs(SSTA_{CTR}] \quad (2)$$

In the expressions above, the subscripts *CTR*, *C*, and *W* refer to control (i.e., observed SST), cold and warm experiments, respectively, and *SSTA* is the observed SST anomaly field for December 2002, January and February 2001. The terms cold and warm in these expressions are related to the control run and not to the observed SST climatology. The absolute value of the SST anomalies is considered for the SST field used in the control run in order to guarantee positive (negative) difference between the SST field of warm (cold) and control experiment over the entire basin. In the warm (cold) experiment, SST anomalies over South Atlantic are nearly 2ºC greater (smaller) than control run. The SST increments were imposed over the South Atlantic Ocean considering the first EOF mode of SST as determined by Venegas et al. (1997) with COADS data set. This mode shows uniform polarity over most of the basin.

The SST field from NCEP was used as surface ocean boundary condition in the two controls run. These runs are referred as *CTRK* and *CTRA* for Kuo and RAS convection schemes, respectively. The other experiments used a negative and a positive increment added to the South Atlantic Ocean (from 40ºS to Equator and 50ºW to 20ºE) and observed global SST in the remaining oceans (Fig. 1b, c). These experiments are referred as *CK* and *WK* for Kuo simulations and *CA* and *WA* for RAS simulations. The AGCM was integrated for 120 days, with 5 distinct initial conditions from the NCEP operational analysis for 12:00 UTC on 1 November 1995, 1996, 1998, 1999 and 2000. These initial conditions are chosen arbitrarily. The December to February (DJF) ensemble averages for each experiment are analyzed.

3. Results

Figure 1 (page 17) shows the rainfall patterns of the *CTRK, CK, WK, CTRA, CA* and *WA* experiments. The cold experiments show decrease of rainfall over the South America for both convection schemes (Fig. 1b and 1e), being more intense for the RAS scheme when compared to the control (Fig. 1a and 1c), particularly over the southeastern and southern part of northeast Brazil. This result suggests that in the CPTEC AGCM the rainfall variability is more sensitive to the cold SST anomalies over the South Atlantic Ocean for the RAS scheme. A possible explanation for this result is that in the CPTEC AGCM with RAS scheme the surface proprieties have an excess weight, with the free condensation level lower in this region or this scheme is less sensitive to the reduced moisture convergence and evapotranspiration with cold SST anomalies over South Atlantic. However, the rainfall response to the cold SST anomalies over southeastern and southern part of northeast Brazil only differs in magnitude but not in the general distribution for both convection schemes.

In the warm experiments (Fig. 1c and 1f) the rainfall patterns are similar to the control runs (Fig. 1a and 1d) for both convection schemes. However, the rainfall is more intense over the oceanic portion of the SACZ. This result may be associated with the low-level moisture convergence generated by cumulus heating and surface temperature gradients. It could also be related to a negative feedback due to the large-scale destabilization, by adjusting the air temperature near the surface to the prescribed SST values through the surface flux. Another possible explanation for the precipitation increase in the *WK* experiment is because the Kuo scheme is strongly driven by low-level moisture flux convergence, which is related to the SST maximum. Although the moisture source includes the large-scale moisture convergence and surface evaporation, the effect of the latter is much smaller than the former. On the other hand, the RAS scheme is not dependent on low-level moisture flux convergence.

The experiment with Kuo scheme indicates that the warming on the South Atlantic Ocean tends to move the SACZ northward, with maximum convection over the southern part of northeastern Brazil (Fig. 1c). In the RAS experiments the SACZ position is not dependent on the SST anomalies over the South Atlantic (Fig. 1d and f). It is interesting to notice that the *WK* experiment indicates an inverse relationship between the SACZ and ITCZ (Fig. 2c and 2b). An intense SACZ is associated with a weak ITCZ. This association is not observed in the warm RAS experiment (Fig. 1f and 2d). The relationship between SACZ and ITCZ in the Kuo scheme could be associated with the closure assumption that it is based on. However, the divergence in the ITCZ region is observed in both warm experiments. Thus, association between the SACZ and ITCZ could also be related to the anomalous subsidence over the ITCZ region due to the intense northward SACZ in the Kuo scheme.

The above results show that the SST anomalies seem to have influence over the convection on the eastern and central Brazil. However, the SST anomalies over the

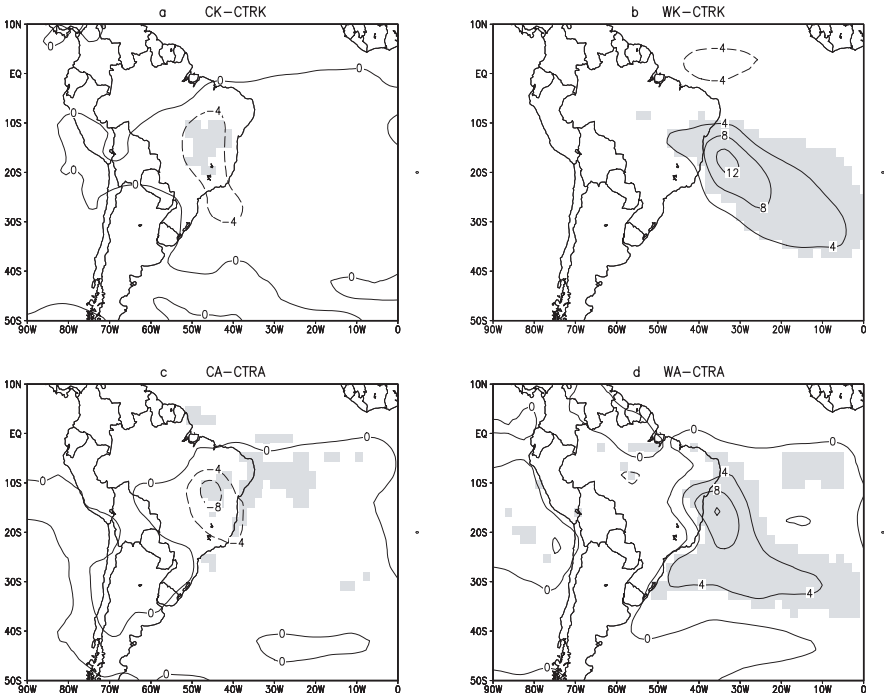

Figure 2 - Rainfall difference (mm/day) between (a) CK *and* CTRK, *(b)* WK *and* CTRK, *(c)* CA *and* CTRA *and (d)* WA *and* CTRA. *The shaded areas represent response significant at the 95% confidence level*

Figure 3 - Rainfall difference (mm/day) between (a) CTRA *and* CTRK, *(b)* WA *and* WK, *(c)* CK *and* CA. *The shaded areas represent response significant at the 95% confidence level*

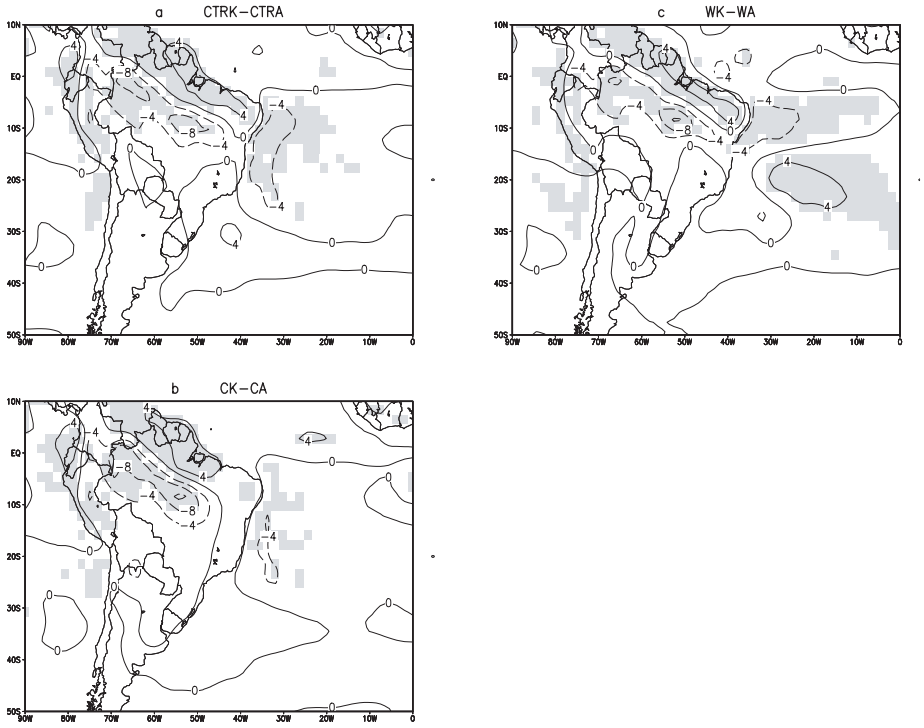

South Atlantic Ocean do not seem to be important for the convection in most of South America. In fact, for the Amazon basin in particular, changes on the SST anomalies or convection schemes affected neither the intensity nor the convection patterns in this region (Fig. 2).

Figure 3 shows the difference between Kuo and RAS schemes for the three experiments. From the comparison of Figures 2 and 3 it is noticed that the change in the cumulus scheme affects the precipitation intensity over most of the continent more than the rainfall response to SST anomalies over the South Atlantic. However, in the eastern South American coastal region the precipitation response to the SST anomalies is more sensitive in the warm experiments. It is possible that the influence of surface processes depends on the extent and distance that separates the land from the ocean.

4. Conclusions

The results obtained show that the decrease (increase) of rainfall over the east of South America and South Atlantic

Ocean is associated with cold (warm) SST anomalies for both convection schemes. Chaves and Nobre (2004) found similar results through numerical experiments with CPTEC/COLA using the Kuo scheme. In addition to the results above, this work showed that the SACZ variability associated with the cold SST anomalies over the South Atlantic Ocean is more sensitive to the RAS scheme than to the Kuo. A possible explanation for this result is that in the CPTEC AGCM with RAS scheme the surface properties have an excess weight or that the condensation free level can be lower in this region. In the RAS experiment the SACZ position seems to be independent of the SST anomalies over the South Atlantic Ocean. However, the warm Kuo experiment indicated an inverse relationship between the SACZ (strong) and ITCZ (weak) systems, which is not observed in the RAS simulation. The results also show that the spatial distribution and precipitation intensity over most of the continent are more sensitive to the convection schemes than to the effect of the SST anomalies over the South Atlantic. However, in the Brazilian coastal area the precipitation response to the SST anomalies is greater than the change in the cumulus scheme, particularly to the warm experiments. This result may occur due to the influence of surface processes, which depend on the extent, and distance that separates the land from the ocean.

Acknowledgments

R. Chaves received financial support from FAPESP (Proc. Nº 03/09259-5). T. Ambrizzi has also received support from FAPESP and CNPq. This Research was partially supported by Inter American Institute for Global Change Research under the process IAI/CRN-055. The authors thank the CPTEC/INPE for the AGCM and use of the NEC/sx-4 supercomputer. A full paper is under revision at the Climate Dynamics journal.

References

Chaves R. R., P. Nobre, 2004: Interactions between sea surface temperature over the South Atlantic Ocean and the South Atlantic Convergence Zone. *Geophys. Res. Lett*. **31:L03204**.

Silva Dias P. L., W. H. Schubert., M. DeMaria, 1983: Large-scale response of the tropical atmosphere to transient convection. *J. Atmos. Sci*, **40**, 2689-2707.

Reaction of the oceanic circulation to increased melt water flux from Greenland – a test case for ocean general circulation models

Rüdiger Gerdes[1], Stephen M. Griffies[2], and William Hurlin[2]
[1]Alfred–Wegener–Institut, Bremerhaven, Germany
[2]Geophysical Fluid Dynamics Laboratory, Princeton, NJ
Corresponding author: rgerdes@awi–bremerhaven.de

Most coupled climate models agree that the thermohaline circulation will slow down due to increased fresh water input in high northern latitudes under increasing greenhouse gas concentrations in the atmosphere (IPCC, 2001). However, the magnitude of the trend differs among models, the sensitivity of the ocean component being the prime candidate for this uncertainty.

This situation motivated the Coupled Model Intercomparison Project (CMIP) to launch coupled experiments where the oceanic component was supplied with an additional fresh water flux in the North Atlantic (R.Stouffer, pers.comm.; www-pcmdi.llnl.gov/projects/cmip/coord_expt.html). It is desirable to conduct corresponding experiments with ocean-sea ice models where atmospheric conditions can be prescribed, allowing to study the effects of anomalous fresh water fluxes in isolation. Furthermore, more detailed ocean models can be utilized than currently used in coupled climate models and parameterizations and other model choices can be varied at smaller computational expense. This note serves to introduce a perturbation experiment designed for this purpose. It forms part of the suite of Coordinated Ocean-ice Reference Experiments (CORE) of the Clivar Working Group on Ocean Model Development (WGOMD). The two other experimental designs of this suite aim at the climatological mean ocean state and the interannually forced response of the ocean or ocean hindcast. Information concerning CORE can be found on the WGOMD web site (http://www.clivar.org/organization/wgomd) and at http://data1.gfdl.noaa.gov/nomads/forms/mom4/CORE.html.

Background

Possible sources of additional fresh water input to the North Atlantic are an enhanced hydrological cycle, the depletion of the Arctic sea ice and fresh water reservoirs, and enhanced melting from Greenland. An enhanced hydrological cycle implies more precipitation over the catchment area of the large Siberian rivers that drain into the Arctic Ocean. The Arctic sea ice volume has been observed (Rothrock et al., 1999) and modelled (Holloway and Sou, 2002; Köberle and Gerdes, 2003) to decrease by a substantial fraction since its maximum in the mid-1960s. Using a simple climate model and a comprehensive thermomechanic model for the Greenland and Antarctic ice sheets for the IPCC96 IS92a scenario, Huybrechts and de Wolde (1999) estimate that by the year 2500, the Greenland ice sheet could loose as much as a third of its volume.

Each source of additional fresh water can provide O(1000km^3/yr) to the Nordic Seas and the subpolar North Atlantic. There are, however, important differences between these sources. The Arctic Ocean fresh water reservoir for instance is limited and can sustain substantial deviation from the average export rates only for decadal to multidecadal time scales. Furthermore, a release from this fresh water reservoir already started three to four decades ago while substantially enhanced precipitation over the Arctic Ocean catchment area and especially the

possible melting of parts of the Greenland ice sheet lie ahead in the future. These latter sources can sustain an enhanced fresh water input to the North Atlantic for a long time.

In equilibrium, the ocean transports fresh water meridionally to compensate for the atmospheric transports. In most ocean basins this is achieved in gyre circulations where salty water is transported from the subtropics to higher and lower latitudes in western boundary currents and relatively fresh water is transported in the interior recirculations. The North Atlantic differs because it has the capability to mix fresh water to large depths. Currently, the Labrador Sea Water receives a large amount of fresh water from the Arctic Ocean and partly the Pacific (through the Bering Strait). This fresh water is carried all the way to the Southern Hemisphere.

What happens when this capability is compromised by additional input of fresh water into the northern North Atlantic? This is the underlying question we wish to answer with "water hosing" experiments as were conducted in the CMIP framework. An issue that is always to be considered for ocean-sea ice coupled models is the proper representation of feedbacks, especially the salt advection feedback that depends on the surface boundary conditions for the ocean-sea ice system. In the following, we will briefly discuss the sensitivity of a specific global ocean-sea ice model under different surface boundary conditions and present a protocol that we submit for a perturbation experiment to complement the climatological and hindcast comparison experiments of the WGOMD-CORE suite.

Surface boundary conditions

A serious problem of perturbation experiments in stand alone ocean-sea ice models is their sensitivity to the form of the surface boundary conditions. For the case of fresh water flux anomaly experiments, the feedbacks involving the atmospheric response to changes in oceanic heat transport are especially pertinent. Ocean models under mixed boundary conditions (effectively the prescription of surface temperature and fresh water fluxes) can exhibit drastically enhanced sensitivity with respect to surface fresh water flux anomalies (Zhang et al., 1993; Rahmstorf and Willebrand, 1995). This is due to the positive salinity advection feedback (Rahmstorf et al., 1996). In nature and in fully coupled models this feedback is partly counterbalanced by the negative temperature advection feedback which is suppressed under mixed boundary conditions. To be operational, it requires a response in atmospheric temperatures to changes in ocean heat transport.

The dependence of OGCM sensitivity on the surface boundary conditions is a general problem as it affects all ocean variability experiments to some degree. Ocean modellers need to find a solution to this problem when future variability experiments should be acceptable to the climate community.

Below, we present four different approaches where the boundary conditions vary from the classical restoring (RESTOR) of surface salinities to climatology to mixed boundary conditions (MIXED) and a method where the salinity consists of two parts of which only one is restored to climatology while an "anomaly" part receives the anomalous fresh water flux and is not damped (SPLIT). The fourth approach is to couple the ocean-sea ice model with an atmospheric energy balance model (EBM). Details concerning the set-up of the boundary conditions and additional results can be found in Gerdes et al. (2005). All experiments carry a tracer S_1 that represents a salinity anomaly directly forced by the anomalous fresh water flux. In the SPLIT experiment this tracer is dynamically active, otherwise it is passive and used for diagnostic purposes. The experiments are accompanied by corresponding control experiments that start from identical initial conditions but do not contain the fresh water flux anomaly around Greenland.

Water hosing experiments

One can anticipate that several fresh water fluxes (strengthened hydrological cycle, reduction of Arctic sea ice and liquid fresh water reservoirs, and melt water from Greenland) will all lead to increased fresh water content in the boundary currents around Greenland. Models that aim at simulating these possible future developments must be able to cope with fresh water flux anomalies that are concentrated in these boundary currents. In our experiments we therefore deviate from the CMIP design where the fresh water flux anomaly was distributed over the latitude band 50°N-70°N in the North Atlantic. The latter choice was partly motivated by numerical considerations that are less compelling in the case of ocean-only models. The fresh water flux anomaly is distributed along the eastern and western coasts of Greenland (between the southern tip of Greenland and Fram Strait on the eastern side and between the southern tip of Greenland and the southern end of Nares Strait at approximately 76°N on the western side). The flux extends 300km into the interior, exponentially decreasing outward from the coast. The total fresh water flux anomaly amounts to 0.1 Sv which is constantly applied over the duration of the experiment. The flux is not compensated by taking fresh water out of the ocean at a different location. In this respect, the fresh water flux anomaly broadly has the properties that we might expect from an increased melt water runoff from Greenland.

In the following experiments, we use GFDL's MOM4 global ocean-sea ice model in the OM2 configuration. (For details see Griffies et al., 2005 and Gerdes et al., 2005. Some features of the model are as follows: tri-polar grid, 2° horizontal resolution, equatorial and high latitude refinement; 50 levels in the vertical; KPP mixed layer scheme; Sweby advection scheme). Atmospheric forcing is provided by the Röske (2001) data set that yields a climatological seasonal cycle with daily variability. It is similar to the Large and Yeager (2004) data set which is recommended for future CORE simulations. To avoid the unrealistic weakening of the meridional overturning circulation (MOC) that occurred in several experiments with this forcing we use enhanced scalar wind over the Labrador Sea. All experiments and the control runs start from the final state of a 100 year integration that follows the CORE protocol for climatological forcing (for the experiments here this is not strictly the case as they were started before the finalization of that protocol). Experiments that use restoring to surface salinities use annual mean values from Steele et al. (2001). The MIXED and EBM experiments are forced with an additional

fresh water flux equivalent to the restoring term, derived from an average over the last 20 years of the spin-up.

The length of the run is chosen as 100 years because major advective adjustments took place only after several decades into the integration. The assumption of a static atmosphere is not valid over such a period. However, the proposed experiment is not primarily designed to realistically describe the climate system's reaction to increased melting of the Greenland ice sheet. The primary purpose is to study the sensitivity of OGCMs and the adjustment processes in response to a certain fresh water flux perturbation without the complication of changes in other forcing fields.

Results

All experiments show qualitatively similar results although huge quantitative differences do exist. The Atlantic MOC weakens (Fig. 1) compared to the control runs. The overturning in the control cases (with prescribed atmospheric temperature and with the atmospheric energy balance model) increase over the duration of the experiment. Compared to the control cases, the RESTOR and SPLIT experiments show a decline of the overturning although its strength is still increasing somewhat during the experiments. EBM and MIXED exhibit a more pronounced drop in the strength of the overturning. Although the temperature advection feedback is only present in the EBM experiment, the differences in the response between EBM and MIXED appear relatively minor over the duration of the experiment.

Although the meridional overturning circulation slows down, it does not completely shut down within the 100 years of the experiment. Thus, the salinity anomaly measured by the tracer S_1 spreads into the Arctic Ocean and the circumpolar deep water of the Southern Ocean as shown for the example of EBM in Fig. 2. The tracer follows the path of the deep western boundary in the model's Atlantic. The signal has reached the ACC and has already been carried through the Indian and Pacific oceans. Large quantities of tracer are also deflected into the Arctic Ocean.

This tracer reflects only the direct effect of the fresh water flux anomaly. In MIXED and EBM, the indirect changes in salinity due to the weakening of the large scale meridional circulation are far greater than the direct effect of the freshwater flux anomaly. Salinity in the subtropical recirculation drops as some of the fresh water is diverted into subpolar and subtropical mode waters. Salinity also drops in all levels of the western subpolar North Atlantic. Initially, the salinity in the upper NADW increases as the supply of relatively fresh Labrador Sea Water is reduced and Mediterranean-influenced water spreads westward. The age of the water in the upper parts of the deep western boundary current increases. However, a fresh North East Atlantic Intermediate Water is formed and reaches the western boundary at 25°N after 90 years and 40 years into the integration for MIXED and EBM, respectively (Fig. 3). No such arrival of fresher water can be seen in RESTOR. In this experiment, no pool of extremely fresh water is formed in the northeastern North Atlantic because of the damping of surface anomalies and the resulting lack of response in the large circulation.

Final remarks

Forcing ocean-sea ice models with a fresh water flux anomaly around Greenland gives the opportunity to study the adjustment processes of the large scale oceanic circulation and the effect of the thermohaline circulation on the hydrographic state, sea level distribution, and heat transports. In two experiments without a restoring to surface salinity climatology, the large scale circulation changes significantly, resulting in Atlantic wide salinity anomalies that by far surpass the anomaly induced by the imposed anomalous surface fluxes. While changes in the North Atlantic and the Arctic are largest, the effect of a weakened thermohaline circulation can be observed in the changed meridional salinity gradient, a fresher North Pacific, and in the exchanges between the Southern Ocean and southern mid-latitudes. For these purposes, the simple approach using mixed boundary conditions is sufficient and recommended for the third component of the CORE suite of experiments.

Another topic of interest, the sensitivity of the ocean-sea ice component in coupled climate models is not easily addressed in such experiments because ocean-sea ice models experience different feedbacks from their counterparts in coupled climate models. Depending on surface boundary conditions, we found a large range of sensitivity to fresh water flux perturbations in the northern North Atlantic in a global ocean-sea ice model.

While changes in wind stress and the atmospheric water transports will probably change the results obtained with a simple atmospheric component, results from partially coupled climate models (Dixon et al., 1999; Mikolajewicz and Voss, 2000) indicate that at least the effect of changed wind stresses might be of minor importance compared to that of the surface heat flux changes. It seems to be necessary and worthwhile to develop and improve simple atmospheric components to be used in ocean-sea ice experiments with variable or anomalous forcing. The CORE experiments can provide a common experimental frame work to compare and validate such efforts.

References

Dixon, K.W., T.L.Delworth, M.J.Spelman, and R.J.Stouffer, 1999: The influence of transient surface fluxes on North Atlantic overturning in a coupled GCM climate change experiment, *Geophysical Research Letters*, **26,** 2749-2752.

Gerdes, R., W.Hurlin, and S.M.Griffies, 2005: Sensitivity of a numerical model of the global ocean circulation to increased melt water flux from Greenland (in preparation).

Griffies, S.M., A. Gnanadesikan, K.W. Dixon, V. Balaji, W.F. Cooke, T.L. Delworth, J.P. Dunne, R. Gerdes, M.J. Harrison, I.M. Held, W.J. Hurlin, H.C. Lee, Z. Liang, G. Nong, R. C. Pacanowski, A. Rosati, J. Russell, B.L. Samuels, M.J. Spelman, R.J. Stouffer, C.O. Sweeney, M. Winton, A.T. Wittenberg, F. Zeng, R. Zhang, 2004: GFDL's CM2 Global Coupled Climate Models: Ocean Model Formulation. (in preparation)

Holloway, G., and T. Sou, 2002: Has Arctic sea ice rapidly thinned? *J. Climate*, **15**, 1691–1701.

Huybrechts, P., J. de Wolde, 1999: The dynamic response of the Greenland and Antarctic Ice sheets to multiple-century climate warming, *J.Climate*, **12**, 2169-2188.

IPCC, Climate Change 2001: The scientific basis. Contribution of working group I to the third assessment report of the Intergovernmental Panel on Climate Change, edited by J.T.Houghton, Y.Ding, D.J.Griggs, M.Noguer, P.J.van der Linden, X.Dai, K.Maskell, and C.A.Johnson, Cambridge University Press, Cambridge, U.K., 881 pp.

Köberle, C., and R. Gerdes, 2003: Mechanisms Determining the Variability of Arctic Sea Ice Conditions and Export, *J.Climate*, **16**, 2843-2858.

Large, W.G. and S.G. Yeager, 2004: Diurnal to decadal global forcing for ocean and sea-ice models: the data sets and flux climatologies, CGD Division of the National Center for Atmospheric Research, NCAR Technical Note: NCAR/TN-460+STR.

Mikolajewicz, U. and R.Voss, 2000: The role of the individual air-sea flux components in CO2-induced changes of the ocean's circulation and climate, *Climate Dynamics*, **16,** 627-642.

Rahmstorf, S., and J.Willebrand, 1995: The role of the temperature feedback in stabilizing the thermohaline circulation, *J.Phys.Oceanogr.*, **25,** 787-805.

Rahmstorf, S., J.Marotzke, and J.Willebrand, 1996: Stability of the thermohaline circulation. In: The warmwatersphere of the North Atlantic, W.Krauss (Ed.), Borntraeger, Berlin, 129-157.

Röske, F., 2001: An atlas of surface fluxes based on the ECMWF reanalysis—A climatological database to force global ocean general circulation models. Report 323, Max-Planck-Institut für Meteorologie, Hamburg, Germany, 31 pp.

Rothrock, D. A., Y. Yu, and G. A. Maykut, 1999: Thinning of the Arctic sea-ice cover. *Geophys. Res. Lett.*, **26**, 3469–3472.

Steele, M., R. Morfley, and W. Ermold, 2001: PHC: A global ocean hydrography with a high-quality Arctic Ocean. *Journal of Climate*, **14,** 2079-2087.

Zhang, S., R.J.Greatbatch, and C.A.Lin, 1993: A reexamination of the polar halocline catastrophe and implications for coupled ocean-atmosphere modeling, *J.Phys.Oceanogr.*, **23**, 287-299.

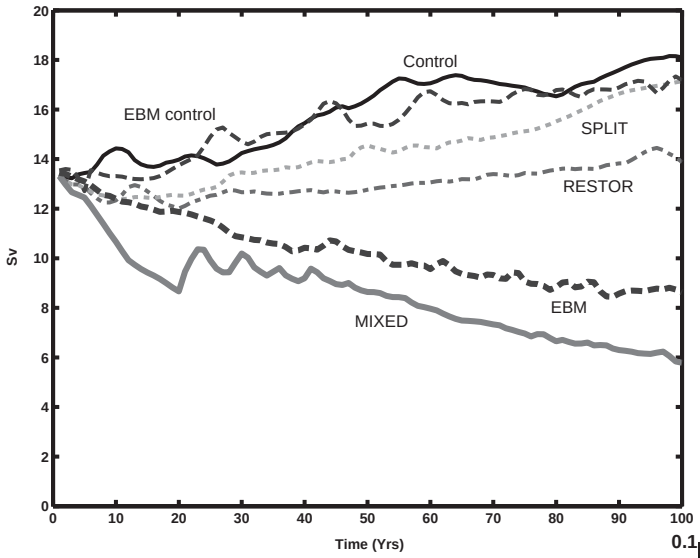

Fig. 1 Strength of the Atlantic MOC. The control cases with prescribed atmospheric temperature and EBM show increasing overturning over the duration of the experiment. Compared to the control cases, the RESTOR and SPLIT experiments show a decline of the overturning. EBM and MIXED exhibit a pronounced drop in the strength of the overturning.

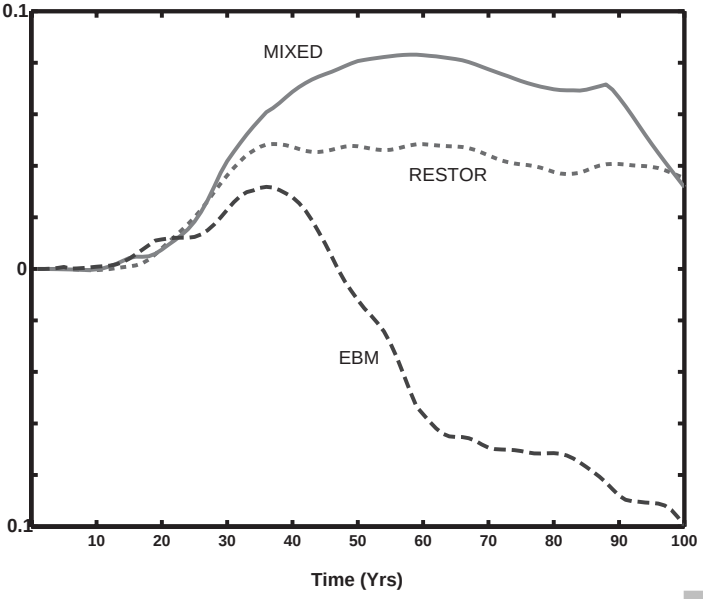

***Fig. 3**. Salinity anomaly (compared to control experiment) for LSW at 25°N. The salinity has been averaged between 75 and 65°W and then the minimum over the depth interval 0:5500m has been taken. All experiments show an initial increase in salinity as more saline water from the central Atlantic flows into the western boundary layer. However, EBM and MIXED both show the arrival of an extremely fresh intermediate water at the western boundary after 90 and 40 years, respectively.*

Contents

The CLIVAR Newsletter Exchanges is published by the International CLIVAR Project Office
ISSN No: 1026 - 0471

Editor: Howard Cattle
Layout: Sandy Grapes

CLIVAR Exchanges is distributed free of charge upon request (icpo@noc.soton.ac.uk)

If undelivered please return to:
International CLIVAR Project Office
National Oceanography Centre, Southampton, University of Southampton Waterfront Campus, European Way, Southampton SO14 3ZH, United Kingdom